Universidad del País Vasco
Euskal Herriko Unibertsitatea

KIMIKA FAKULTATEA
FACULTAD DE QUÍMICA

Universidad del País Vasco/Euskal Herriko Unibertsitatea

Facultad de Química/Kimika Fakultatea

Kimikako gradua

GRADU AMAIERAKO LANA

INFLUENCE OF MOLECULAR WEIGHT ON THE CRYSTALLIZATION OF POLYHEPTALACTONE (PHL)

Egilea: ASIER OLMOS AMONDARAIN

Zuzendariak: Alejandro J. Muller
Miren Agurtzane Mugica

Donostia, 2021ko uztaila

GIPUZKOAKO CAMPUSA
CAMPUS DE GIPUZKOA
Pº. Manuel de Lardizabal, 3
20018 DONOSTIA-SAN SEBASTIAN
GIPUZKOA

ABSTRACT:

The present work studies the characterization of 4 new homopolymers of polyheptalactone (PHL): PHL 15, PHL 35, PHL 66, and PHL 90; focusing on the influence of the molecular weight. These polymers are interesting because they are biodegradable and very similar to polycaprolactone (PCL), with one additional carbon in the repeating unit.

Two main experimental techniques have been used: Differential Scanning Calorimetry (DSC) and Polarised Light Optical Microscopy (PLOM). With these two techniques non-isothermal and isothermal crystallization experiments have been carried out. On the one hand, PLOM has been used in order to study the morphology of the crystals and the crystallization growth kinetics. On the other hand, with the DSC, the main thermal properties of the new polymers and overall crystallization kinetics have been analyzed. Moreover, Transmission Electron Microscopy (TEM) and Wide-Angle X-ray Scattering (WAXS) techniques have provide additional information about polymer morphology.

The main thermal transitions and crystallization kinetics of the four homopolymers have been determined, applying Avrami and Lauritzen and Hoffman theories. Results conclude that these polymers are stable and semycrystalline. Moreover, molecular weight affects in a different way the measured properties. Lamellar thickness and X-ray diffractograms are not affected by the molecular weight while phase transition temperatures and crystallization rates increase when molecular weight rises.

LABURPENA

Lan hau Poliheptalaktonazko (PHL) 4 homopolimero berrien karakterizazioan oinarritu da: PHL 15, PHL 35, PHL 66 eta PHL 90; pisu molekularraren eragina aztertuz. Polimero hauek interesgarriak dira biodegradagarriak direlako eta Polikaprolaktonaren (PCL) oso antzekoak direlako, karbono atomo bat gehiago izanik unitate errepikakorrean.

Nagusiki bi teknika esperimental erabili dira: Ekorketazko Kalorimetria Diferentziala (DSC) eta Argi Polarizatutako Mikroskopio Optikoa (PLOM). Bi teknika hauekin kristalizazio ez-isotermiko eta isotermikoak burutu dira. Alde batetik, PLOM-ren bidez kristalen morfologia eta kristalizazio hazkuntzaren zinetika aztertu da. Bestalde, DSC-ren bidez polimeroaren propietate termiko nagusiak eta kristalizazio osoaren zinetika aztertu dira. Gainera, Transmisio Mikroskopio Elektronikoa (TEM) eta Angelu Zabaleko X-izpi Sakabanaketa (WAXS) teknikek polimeroaren morfologiari buruzko informazio gehigarria eman dute.

4 homopolimeroen trantzisio termikoak eta kristalizazio zinetika determinatu dira, Avrami eta Lauritzen and Hoffman teoriak erabiliz. Emaitzak aztertuz, polimeroak egonkorrak eta semikristalinoak direla ondorioztatu da. Honetaz gain, pisu molekularrak modu desberdinean eragiten du neurtutako propietate eta parametroetan. Lamela lodiera eta X-izpien difraktogramak ez dira aldatzen pisu molekularraren arabera. Fase trantzisio tenperaturak eta kristalizazio abiadurak aldiz pisu molekularrarekin batera handitzen dira.

INDEX

1-INTRODUCTION

1.1 OBJECTIVES

The aim of this work is to study the inffluence of molecular weight on the crystallization of four new semycrystalline polymers of Poly(η-heptalactone) (PHL), exactly, PHL 15, PHL 35, PHL 66 and PHL 90. These polymers were syntheized by B. Li from the University of Birmingham. PHL is very similar to Polycaprolactone (PCL) but there is almost no research about it, so it is interesting to study the crystallization of this new polymer to see if it behaves as other common semicrystalline polymers. Two main experimental techniques have been used: Differential Scanning Calorimetry (DSC) and Polarized Light Optical Microscopy (PLOM).

PLOM has been used in order to visualize the morphology of the crystals that are formed during the crystallization process under non-isothermal and isothermal crystallization conditions. Apart from that, obtaining the crystal growth kinetics has been another important objective of this work.

With the DSC, non-isothermal crystallization experiments have been carried out to determine main phase transition temperatures, as well as other polymer properties, such as crystallinity degree (X_c). Besides, applying isothermal crystallization experiments the overall crystallization kinetics can be determined.

Transmission Electron Microscopy (TEM) and Wide Angle X-ray Scattering (WAXS) have been used to obtain information about the crystal morphology.

Moreover, this project focuses on the comparison of the results obtained for the four homopolymers, specially in how the molecular weight affects in the different measured parameters.

1.2 BIOPLASTICS AND POLYESTERS

1.2.1 Bioplastics

Nowadays, plastics are one of the most used material due to their versatility, manufacturability and its low cost of production. Inside this family there are many types of plastics that have a wide range of properties. For this reason, plastics can be found in almost all production sectors, such as, packaging, clothing, paints, medicine or electronics.

However, the massive production and use of plastics has carried out one of the biggest problem of the current issues: plastic waste. Apart of that, most of the plastics are obtained from oil fossils. Therefore, this type of plastics increase the emissions of CO_2 into the atmosphere and get worse the climate change.[1]

One solution to this problem could be to use bioplastics. There are three type of bioplastics: bio-based, biodegradable or both bio-based and biodegradable, as it is shown in figure 1.1

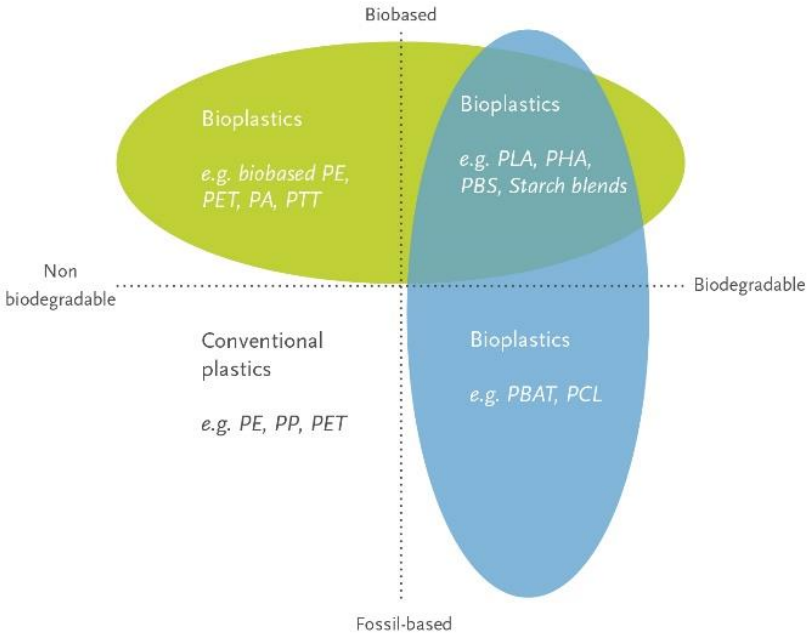

Figure 1.1 Type of bioplastics: Biobased, biodegradable or both.[2]

Biobased polymers are obtained from biomass, which can be natural polymers like celullose or their monomers are derivatives of renewable resources like corn or sugars. Besides, a biodegradable polymer is a polymer that, following exposition to microrganisms, can desintegrate naturally into biogases and biomass.[3]

These two main characteristics of bioplastics can be the solution to the problems related with the traditional oil-based polymers. Thus, Investigation and use of bioplastics has gone up during the last years. It is predicted that this tendency will continue and in 2025 the production of bioplastics will increase a 36%, as it is shown in the figure 1.2. [2]

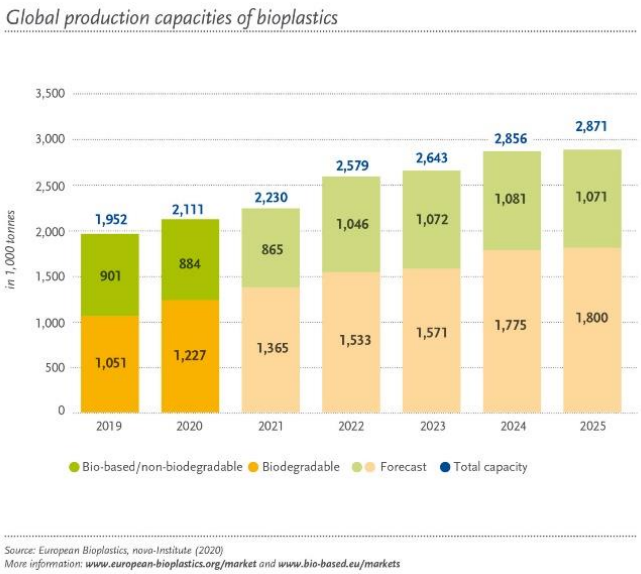

Figure 1.2. Estimated annual production of bioplastics for the following years.[2]

Nevertheless, in 2020, bioplastics did not even arrive to the 1% of all plastic production.[2] Therefore, one of the most important current challenges in polymer science, especially in the area of reserch, is the development of bioplastics that can achieve same or superior properties than petroleum based polymers.

1.2.2 Polyesters

Polyesters are polymers that include an ester funtional group in the main chain, as it can be seen in the figure 1.3. Most of them are bioplastics because they are biodegradable and some of them are even biobased. In spite of their high molecular weight are capable of biodegradate thanks to their hydrolysable ester bond. Polyesters are often also biocompatible, so this class of material is suitable for medical and pharmaceutical applications. Moreover, thanks to the huge variety of polyesters and their synthetic versatility, they are one of the most studied and used biodegradable polymers.[4,5]

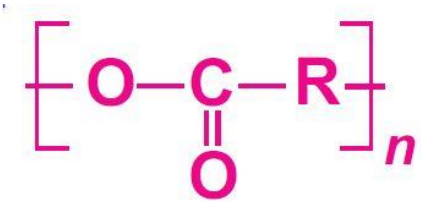

Figure 1.3. Chemical Structure of polyesters.[6]

One of the most common polyester is Polycaprolactone (PCL) which consists on repeated units of hexanoate, as it can be seen in the figure 1.4. It is usually obtained from a ring-opening polymerization, ROP, of ε-caprolactone or from a polycondensation of hydroxycarboxylic acid.

Figure 1.4. Chemical structure of PCL. [7]

Biodegradable and biocompatible PCL is miscible with other polymers and its costs production is very low. These aspects make the PCL one of the most used polymer and it can be found in different fields like tissue engignering, drug delivery systems, packaging or as an additive to polyurethanes. Most of the PCL is petrolium based, but it has potential to be made from monomers that come from renewable sources.[8]

Taking into consideration the advantages of PCL, similar or even better polymer alternatives are being investigated. One chance can be using similar lactones to ε-caprolactone. For example η-heptalactone is a lactone with one more carbon unit than ε-caprolactone in the main chain, so it is expected to show similar properties to PCL. However, since η-heptalactone it is not commercially available there is very little research about it, only few ones, like the enzymathic ROP of η-heptalactone using Novozym 435 as a catalist. [9]

1.3 POLYMERS BEHAVIOUR DURING CRYSTALLIZATION PROCESS

Crystallization is a thermodynamic phase transition which involves a change in the molecules structure. It is very characteristic of polymers, but also of another materials such as metals or ceramics. The field of polymer crystallization has been studied for many years but nowadays is still an active research field.[10]

1.3.1 Amorphous and crystalline polymers

Polymers can be classified in amorphous or semi-crystalline depending on the order of its chains. On the one hand, semi-crystalline polymers have chains that are packed together more efficiently and tightly so they have higher density than amorphous. On the other hand, amorphous materials are not capable of order since they usually do not have a structural regularity and simetry before lowering the temperature.

As it will be explained later, polymers cannot be 100% crystalline because of their long chains so it is better to use the term semi-crystalline. Being semi-crystalline or amorphous will determine strongly its final properties. [11]

1.3.2 Crystalline morphologies

Depending on the starting point of the crystallization different types of crystal morphologies are formed. If the crystallization is done from solution single crystal lamellae are formed. If this process takes part from the melting state, usually special structures called spherulites are obtained. This two structures are of different dimension and, consequently, different techniques are used to analyze them.

a) Crystallization from solution: *single crystal lamellae*

During history different models for crystallization structures have been presented. At the beggining of the 20th century a **fringe micell model** was suggested. This model states that some chains form several crystalline structures that were in a matrix of amorphous materia. This model explained some properties of the polymers but not all.

Some years later, during some electron diffraction experiments it was noticed that the chains were parallel to the shortest dimension of the lamellae, which is the thickness. Therefore it was suggested that the polymer´s chains fold back and forth upon themselves in a very accurate way to maintain the lamellae thickness and the surface in perpendicular way. This model is called **chain folded model,** which is shown in the figure 1.5. Lamellae thickness is usually affected by the crystallization temperature.

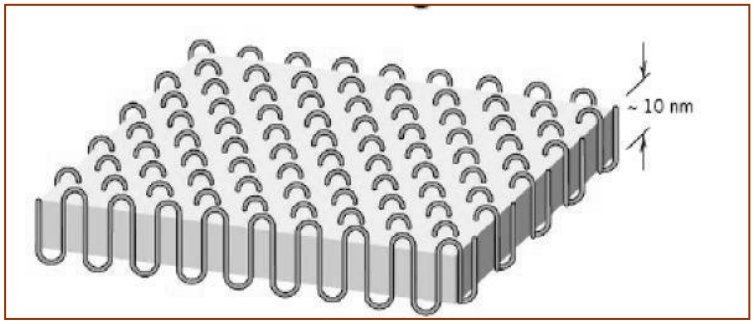

Figure 1.5 Chain folded model of a lamella.[12]

As it has been explained before, semycrystalline polymers contain amorphous material between the lamellae. In the lamellar surface it is accepted that the folded part of the chains are in the amorphous state.[10]

b) Crystallization from the melt: *spherulites*

Crystallization from the melt is different to the crystallization from solution, but it is very important since most of the processes in industry are performed with melt crystallization. For concentrated solutions the same process is suggested.

In the crystallization from the melt, the chains are entangled with one another in high molecular weight polymers and it is more difficult to form isolated structures as the viscosity of polymer is high. Instead of that, crystals aggregates form structures called spherulites.

Lamellae grow radially from the centre of the spherulite forming a spherical structure. These spherulites are formed of several lamellaes that grow in a perpendicular way to the radius of the spherulites. In the space between the lamellaes there is amorphous materia, as it is shown in the figure 1.6.

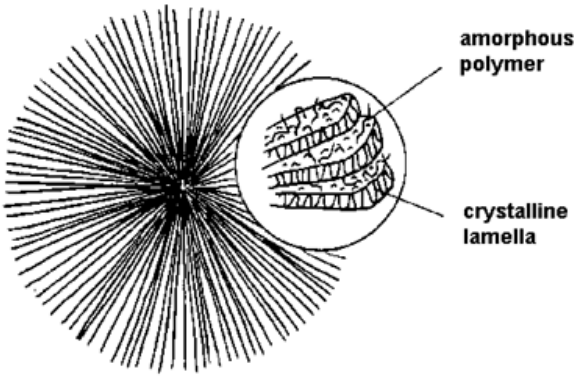

Figure 1.6. Structure of a spherulite.[13]

At the beginning the spherulites are not totally spherical and they have an extended form, but during the growth the lamellae starts branching out and finally obtain a circular shape. The process is shown in the figure 1.7. Llamellae usually grow around all space forming three dimensions spherulites, although crystals of two and one dimensions also exist. Spherulites continues growing until they collapse between them. It is important to take into account that spherulites and single crystal lamellae have very different size since spherulites are formed of several lamellaes.

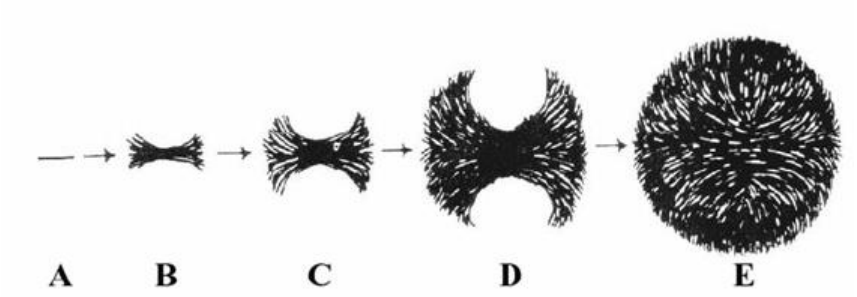

Figure 1.7 Growth of a spherulite.[14]

As the same way that the crystallization temperature affected the thickness of the lamellae the crystallization temperature has effect in the number and size of spherulites. When the temperature is lower, spherulites density is usually higher and they are smaller. [15,16]

1.3.3 Crystallization phases

Crystallization of polymers can be divided in two phases: primary crystallization, which starts with the creation of a nuclei and finishes when the spherulites collapse between them and secondary crystallization where complementary crystal growth happen.

Primary crystallization is divided also in two process: nucleation and growth.

a) **Primary nucleation:** In this process it is created a nuclei that later will become a crystal. The nuclei needs a critical size and a minimum free enthalpy value to start growing, otherwise the nuclei will dissapear from the system. Both critical size and free enthalpy barrier decrease while the crystallization temperature is lowered.[15]

Theoretically there are two types of nucleation. On the one hand, if the nuclei is formed from molecules or material of the polymer itself it is called **homogenous nucleation**. On the other hand, if the nucleation happens in the presence of any external particle such as, catalyst rests, nucleation agents or dust, it is called **heterogenous nucleation**. Experimentally heterogenous nucleation prevails on the homogenous one since is thermodinamically favoured. In some cases, the nuclei precursor is a nuclei formed in a previous crystallization, which is called **self nucleation**.[17]

Moreover, taking into account the time that a nuclei need to be created, there are two types of nucleation. In the **instantaneous nucleation** several activated nuclei appear at the same time because the nucleation rate is higher than the growth rate. Hence, the spherulites are small but the density is high. This happens when crystallization temperature is low. In the **sporadic nucleation**, as the growth rate is higher than the nucleation rate less spherulites are created but the size of them is bigger.

Primary nucleation is very important since it determines strongly the properties of the material. In fact, abundant and small spherulites enhance optical and mechanical properties, which ocurrs in instantaneous nucleation. [15]

b) **Growth or secondary nucleation:** After the creation of a stable nuclei it starts the radial growth in order to form a spherulite. In the crystal growth two different processes are implied: molecular transport or diffusion of the molecules to the nuclei and the growth of the nuclei. This two process are afected by the temperature but in a different way. On the one hand, diffusion is favoured at higher temperatures since approaching to the glass transition temperatures the chains loss mobility. On the other hand, the growth of the nucleis is favoured

with lower temperatures. Therefore, the temperature of the maximum growth rate is usually in the middle of T_g and T_m.[18]

Two types of growth happen simultaneously: surface nucleation, where molecules are added to the nuclei surface and lateral spreading growth, where the crystal expanded laterally. Temperature will dominate the rate of each process and hence the morphology of the spherulite.

At high temperatures, there are not many activated nuclei. In this case, the lateral growth rate, g, is higher than the surface nucleation rate, i. As a result, before a new nuclei is activated the previous activated nuclei has grown laterally. In this case the spherulite is not so spherical and takes two dimenssions, which it is called axialite.

At intermediate temperatures, there are more activated nuclei. i and g are similar and the morphology of the crystal is a ringered spherulite.

At low temperatures, i is higher than g, so crystal growth even happens only with surface nucleation, which ocurrs in the diferent planes. The morphology of the crystal is a fibrilar spherulite.[10]

Since many spherulites grow at the same time, they collapsed between them and at that point **secondary crystallization** starts. Crystallization slows down and another complementary processes such as crystallization of material between spherulites, thickening of lamellaes or perfection of the crystals happen. However, this process is still unknown and there are doubt about its mechanism.[19]

1.3.4 Thermodynamics and kinetics of crystallization

Crystallization is driven by two forces: thermodynamics and kinetics. Thermodynamics conditionate under specific circumstances if crystals can exist or not, which happens in the primary nucleation.[18]

A process is thermodynamically favoured when Gibbs free energy, G, is reduced. G can be calculated with the equation 1.1:

$$G = H - TS \ (\boldsymbol{Eq\ 1.1})$$

Where H is enthalpy, T is temperature and S is entropy. Chains packaging into crystalline structures provides an enthalpy and Gibbs free energy reduction. Therefore, chains prefer to form crystals than to be isolated.

However, whether crystallization takes place and its speed is determined by the kinetics of the process. If all the crystallization process will be dominated by thermodynamics, infinite long crystals will be formed, which does not occur. Therefore crystalls are limited and polymers cannot crystallize 100% as it has been mentioned before.[10]

There are different theories that analyze crystallization kinetics, and two important ones are Avrami theory and Lauritzen and Hoffman theory, LH. [10]

a) Avrami theory

Avrami theory is based on the following equation:

$$1 - V_c \ (t - t_0) = \exp(-k \ (t - t_0)^n) \ (\boldsymbol{Eq\ 1.2})$$

Where V_c is the relative volumetric transformated fraction, or in another words, the proportion between crystalline and amorphous phase; t is experimental time, t_0 is induction time, which is the time that need a supersaturated solution to reach the onset of nucleation[20]; k is the overall crystallization rate constant and n is avrami index.[21] V_c can be calculated as follows:

$$V_c = \frac{W_c}{Wc + \left(\frac{\rho_c}{\rho_a}\right) * (1 - W_c)} \ (\boldsymbol{Eq\ 1.3})$$

Where W_c is the crystalline mass fraction; ρ_c and ρ_a and are the density of the crystalline and amorphous phases respectively. W_c can be calculated knowing the ΔH (t), the crystallization enthalpy at an exact time and the $\Delta H_{total,}$ which is the overall enthalpy at the end of the crystallization, as it is in the equation 1.4:

$$Wc = \frac{\Delta \mathrm{H(t)}}{\Delta \mathrm{H_{total}}} \ (\boldsymbol{Eq\ 1.4})$$

Plotting log(-ln(1-V_c)) versus log(t-t_0) a linear graph should be obtained. From that graph, two important parameters can be obtained: n, which is the slope of the function, and k, which is the intercept.

Avrami index (n) is an important crystallization parameter since it gives information about the crystallization process and morphology. Avrami index is the sum of two types of avrami index, as it can be seen in the following equation:

$$n = n_d + n_n \ (\boldsymbol{Eq\ 1.5})$$

n_d represents in how many dimension is growing the crystal, that can be one, which the morphology will be a road two, which will be an axialite or three, which will be an spherulite, the most usual one.

On the other hand n_n expresses if the nucleation is instantaneous, with a value of 0 or sporadic with a value of 1.

Another important crystallization parameter is the crystallization half-time, $\tau_{\%50}$, which is the required time to achieve a 50% relative conversion to the semi-crystalline state in the polymer. It can be calculated with the Avrami equation taking into account that V_c will be 0.5.[18,11]

b) Lauritzen and Hoffman theory

Lauritzen and Hoffman theory, LH, is another important theory to analyze crystallization kinetics. In spite of being one of the first theories in this area is still useful in some aspects. Depending on the experimental technique used, growth crystallization kinetics (PLOM) or overall crystallization kinetics (DSC) can be analyzed. Overall crystallization kinetics involves both nucleation and growth processes.

In the secondary nucleation, the main parameter is the growth rate, G, which analyzes the velocity during the growth of the crystal. According to the LH theory, G can be expressed with the following equation:

$$G(T) = G_0 \exp\left(\frac{-U^*}{R(T_c - T_\alpha)}\right) \exp\left(\frac{-K_g^G}{T_c \Delta T_f}\right) \quad (\boldsymbol{Eq\ 1.6})$$

G_0 is a preliminar growth constant. Each exponential is related with the two processes that involve the crystal growth: diffusion and secondary nucleation. The first exponential rely on the diffusion, where, U* is the activation energy needed to transport the molecules to the growth front, R is the gas constant, T_c is the crystallization temperature and T_α is the temperature at which there is no chain mobility, usually calculated doing T_g-30°K. The second term, is a secondary nucleation term determined by K_g^G, a parameter proportional to the energy barrier that has to be crossed for growth, T_c which is crystallization temperature, ΔT which is the supercooling, and f, which is a thermal correction term. However, following crystallization growth in the PLOM G can be calculated manually.

When overall crystallization kinetics is analyzed it is not used growth rate, instead of that it is used overall crystallization rate (which includes primary nucleation and growth), $1/\tau_{\%50}$. Hence, LH theory can be rewritten in the following way:

$$\frac{1}{\tau_{50}\%}(T) = G_0^{\tau} \exp\left(\frac{-U^*}{R(T_c - T_\alpha)}\right) \exp\left(\frac{-K_g^{\tau}}{T_c \Delta T_f}\right) (\boldsymbol{Eq\ 1.7})$$

It is very similar to the equation equation 1.6, but the elements that have τ means that the parameter has been measured with the DSC.[18,22]

1.4 PHASE TRANSITIONS

All phase transitions are not thermodinamically the same and the two more important ones are first and second order transitions.

Gibbs free energy, G, express the possibility to happen a process spontaneously. G is affected by the temperature, T, and the Pressure, P, with the following equation:

$$dG = -SdT + VdP\ (\boldsymbol{Eq\ 1.8})$$

The first derivative at a constant P is related with the entropy while the first derivative at a constant T is related with the volume, according to the following equations:

$$\left(\frac{dG}{dT}\right) P = -S\ (\boldsymbol{Eq\ 1.9})$$

$$\left(\frac{dG}{dP}\right) T = V\ (\boldsymbol{Eq\ 1.10})$$

During a phase transition, the two phases are in equilibrium so there is no ΔG and the ΔS can be calculated with the following equation:

$$\Delta S = -\frac{\Delta H}{T} \ (\boldsymbol{Eq\ 1.11})$$

In a phase transition S changes due to the change between initial and final state so H is going to change too. That H is called heat of transition or latent heat, and is the heat that the system absorbes during a phase transition. In that interval of time, the temperature of the system does not increase because all the heat absorved is used to change of phase.

On the other hand, second derivatives of G are related with the heat capacity, c_p, which is the capacity of heat absorption while temperature is changing; thermal expansion coefficient, α, and compressibility coefficient, β.

In conclusion, **first order transitions** happens when there is a discontinuity in the first derivative of G which is related with the heat transition. As it can be seen in the figure 1.8, in the phase transition temperature heat is exchanged but temperature does not increase.

Example of first order transitions are **melting** and **crystallization** temperatures which only happen in crystalline domains, so in amorphous polymers will not occur these transitions. These two process are the opposite, in the melting the ordered structure dissapears while the temperature increases whereas in crystallization the molecular chains are packaged forming a structured area.

On the other hand, **second order transitions** do not show any discontinuity in the first derivative since heat transition is not involve in the process. However, c_p, α and β changes so the second derivate show a discontinuity. This can be seen in the figure 1.8 since after the glass transition the slope of the function, c_p, change.

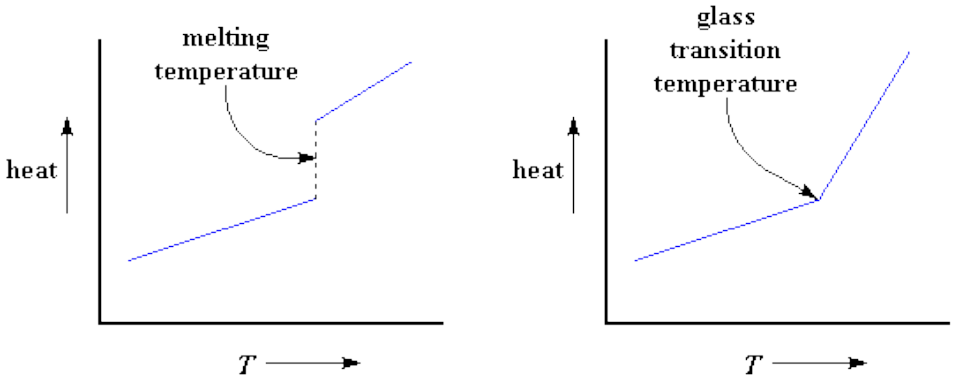

Figure 1.8 Difference between a first order transition (melting) and second order transition (glass transition).[23]

Glass transition, T_g, behaves like a second order phase transition. T_g, is very important since properties change remarkably at this point. Under the T_g the molecule chains do not have mobility so the polymer is rigid. In contrast, above the T_g it happens a conformation change that makes possible the mobility of chains and the polymer behave as a rubber, with an increase of flexibility.[22]

Glass transition can be explained with the concept of free volume. This type of volume is the space between the chains of a polymer, which is empty. Free volume will determine the mobility of the chains. As it is known, when the temperature of a material increases the volume also increases, depending on the thermal expansion coeficient, α. Above T_g free volume increase a lot, so free volume proportion enlarge and the chains are able to move easier.

It is set that T_g is the temperature at which the free volume is the 2.5% of the total volume of the polymer. However, depending on the cooling rate T_g will be different. As the cooling rate is higher it will arrive firstly to phase transition so the T_g will be higher. This phenomenon is shown in the figure 1.9 [24]

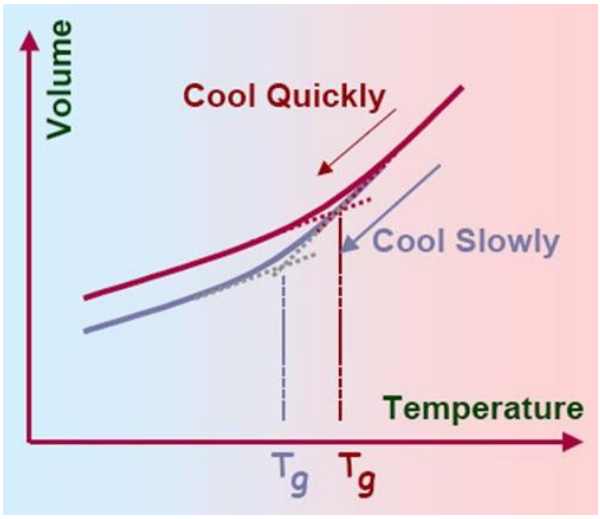

1.9 The effect of cooling rate in the T_g.[25]

2-MATERIALS AND EXPERIMENTAL TECHNIQUES

2.1 MATERIALS

In this project four different homopolymers of Poly(η-heptalactone) (PHL) have been studied: PHL 15, PHL 35, PHL 66 and PHL 90. Each number makes reference to the number of repeating units of η-heptalactone, in other words, the molecular weight. The general structure for PHL homopolymers is shown in the figure 2.1.

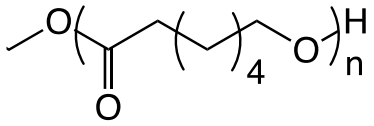

Figure 2.1. General structure of the homopolymers of PHL.

2.1.1 Synthesis

The synthesis of the four homopolymers was carried out by B. Li from the University of Birmingham. PHL was obtained from a ring opening polymerization of the monomer η-heptalactone. As this monomer is not commercially available it was synthesised by Baeyer-Villiger oxidation following a literature procedure[9], which it is shown in the figure 2.2.

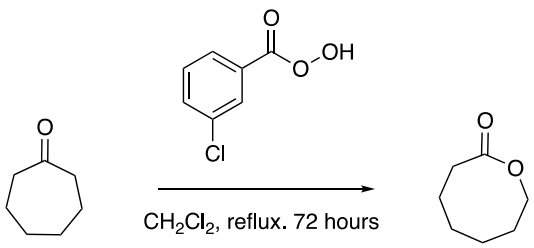

Figure 2.2 Baeyer-Villiger oxidation of cycloheptanone in order to synthesise η-heptalactone.

For the synthesis of the homopolymers a Ring Opening Polymerization, ROP, of η-heptalactone was carried out. Diphenyl phosphate (DPP) was selected as the catalyst and the polymerisation was initiated by a dual-head initiator and chain transfer agent, as it can be seen in the figure 2.3:

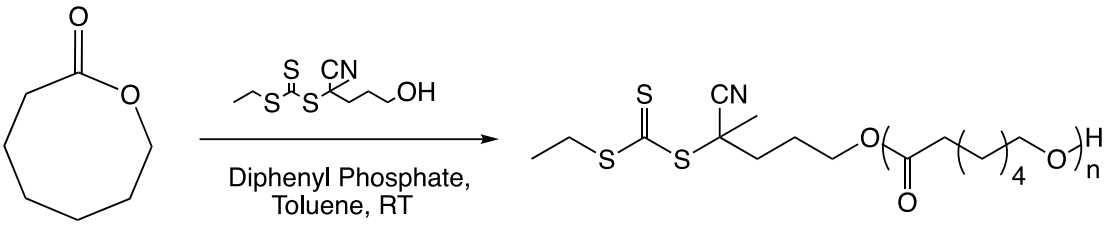

Figure 2.3. Synthesis of the PHL polymers by a ROP of η-heptalactone catalysed by DPP.

Depending on the reaction time different conversion was obtained and therefore four different homopolymers were synthesized with their corresponding molecular weight. Molecular weight was measured by H NMR and the data can be seen in the table 2.1:

Table 2.1 Time needed for the polymerization reaction of each homopolymer and the corresponding molecular weight.

Time (h)	Homopolymer	Mn (NMR) (g/mol)
1	PHL 15	2200
2	PHL 35	4700
4	PHL 66	9200
5	PHL 90	11800

2.2 EXPERIMENTAL TECHNIQUES

In this project, different techniques have been used to analyze the four homopolymers. The study has focused on the use of Differential Scanning Calorimetry (DSC) and Polarised Light Optical Microscopy (PLOM), but to obtain additional information Transmission Electron Microscopy (TEM) and Wide-Angle X-ray Scattering (WAXS) have been employed too. It has to be taken into account that each technique is used to analyze in a different scale the crystalline morphology and structure of the polymer, as it can be seen in the figure 2.4:

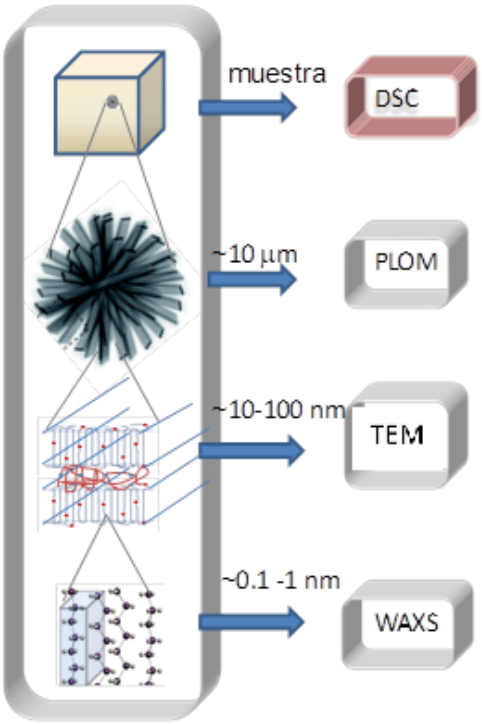

Figure 2.4. Experimental techniques used to analyze the polymer and their corresponding scale.

From the point of view of polymer crystallization, WAXS analyze polymer crystallization with the lowest scale, since it gives information about the unit cell of the crystal. TEM is focused on the lamellaes that are form by the folding of the chains and the domain is between 10-100 nm. PLOM analyze the formation of spherulites, which are formed of several lamellaes, so the scale is bigger. Finally DSC studies the overall polymer crystallization, because it measures the heat that the sample exchanges during this process.

2.2.1 Polarized Light Optical Microscopy (PLOM)

2.2.1.1 Theoretical basis

This optical technique is very useful to study the morphology of the polymer crystallization, but also the kinetics of the spherulites, since the growth can be followed in front of the time.

The PLOM is a typical microscope which has two additional polarizing filters called polarizer and analyzer. These two filters are in a perpendicular way. A polarization filter only allow to pass a light with a determined plane and like this polarized light is formed. Because of that, polarizer is put before the sample so that polarised light attack the sample. This type of light behaves differently if the sample is anisotropic or isotropic.

Characteristics of isotropic materials do not depend on the orientation. Polarized light passes through the sample and its direction does not change, so the light arrives to the analyzer in a perpendicular way. Therefore, no light will go through the analyzer and dark image is seen. Nevertheless, if the material is anisotropic, where the characteristics of the material will change depending on the orientation, the polarized light is split into two different perpendicular rays: ordinary ray and extraordinary ray. These two rays have difference velocity and different refraction index. The difference between this two refraction index is called birefringence. In this case, as the ordinary and extraordinary rays are perpendicular, one of them will pass through the analyzer and an image will arrive to the eyepiece, as it can be seen in the figure 2.5.

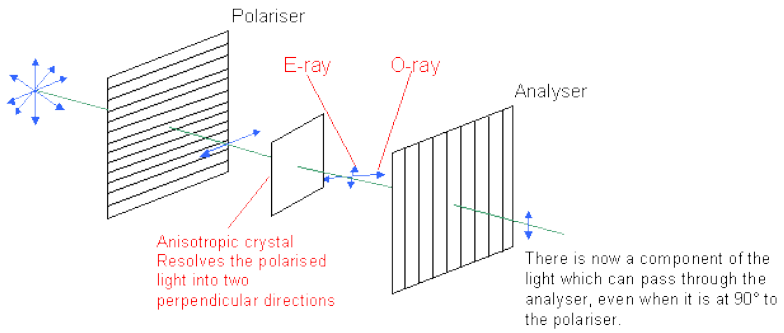

Figure 2.5. A simple scheme of the PLOM.

Polymer crystals are very anisotropic materials since they have strong covalent bonds along the chain axis whereas the cohesion along the lateral is achieve with weaker bonds. Hence, PLOM is a very useful analytical instrument because only crystalline phase can be seen. Therefore, in the PLOM will be seen some colourful figures which are spherulites, as it is shown in the figure 2.6.[26]

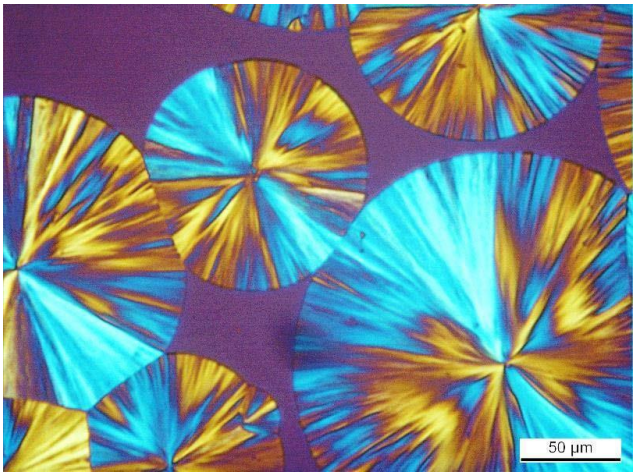

Figure 2.6. Photograph of some spherulites obtained by the PLOM.[13]

As it has been said before, kinetics of the crystallization can be analyzed with this technique. Comparing with the DSC, PLOM only studied the crystallization growth kinetics. For that, it is needed to measure the radius of the spherulite at different times. Plotting radius versus the time, a function is formed and the slope of that function is the Growth rate, G, a very important kinetic parameter.

Applying LH theory, equation 1.6, another kinetic parameters can be obtained: K_g, the energy barrier that has to be crossed to happen the crystallization; σ, which is the lateral free energy; σ_e, which is the fold surface free energy and q which is the work done by the chain to form a fold.

2.2.1.2 Experimental procedure

A polarized light optical microscope, Olympus BX51 (Olympus, Tokyo, Japan), equipped with an Olympus SC50 digital camera and with a Linkam-15 TP-91 hot stage (Linkam, Tadworth, UK) (coupled

to a liquid nitrogen cooling system) was used to observe spherulites crystallization, the one of the figure 2.7.

Figure 2.7. Equipment that was used in the lab: the PLOM, the hot stage and the computer.

To prepare the samples a small quantity of the solid polymer, more or less a rice grain, was melted between two glass slides in order to obtain a film.

Depending on the mode of operation, isothermal crystallization or non-isothermal crystallization, different parameters are measured. In non-isothermal crystallization, crystallization temperature is not constant during the process and it drops with a constant cooling rate. For the non-isothermal crystallization, the following procedure has been used:

1) Heat the sample at 20°C/min until 90°C (T_m + 30°C more or less) and stay 3 minutes at that temperature to erase the previous thermal history of the polymer.
2) Cool down at 20°C/min until the crystallization was ensured, in this case until 25ºC

In isothermal crystallization, crystallization temperature is maintained constant during the crystallization. The isothermal crystallization experiments were performed with the following protocole:

1) Heat the sample at 20°C/min until 90°C and stay 3 minutes at that temperature in order to erase previous thermal history of the polymer.
2) Cool down at 50°C/min, the maximum cooling rate of the used PLOM model, until the selected crystallization tenperature, T_c.
3) Stay at the T_c the required time to measure the crystalls at least at 10 different times.
4) Repeat the same procedure to have in total results of 5 T_c to analyze well kinetics

To choose the adecuate T_c, they were used temperatures at which the size of the spherulites was measurable

2.2.2 Differential Scanning Calorimetry (DSC)

2.2.2.1 Theoretical basis

Differential Scanning Calorimetry, DSC, is one of the most common thermal analysis technique. It is an effective and widely applied analytical tool to measure different physical properties of a polymers, thanks to its simplicity, rapidity, universality, the possibility of being used in a wide range of temperatures and the option to analyze materials in very different forms.[27] Calorimetry is based on the following equations:

$$\Phi = \frac{\delta Q}{dt} \ (\boldsymbol{Eq.2.1})$$

$$\frac{\delta Q}{dt} = mc_p \frac{dQ}{dt} \ (\boldsymbol{Eq.2.2})$$

Where Φ is the heat flow, which can be calculated with a division between the exchanged heat, δQ, and the differential time, dt, m is the mass of the sample, c_p is the heat capacity and dT/dt is the division between the differential temperature and differential time.

DSC is based on differential power between two samples, because of that, apart from the sample under investigation it is needed a reference. The reference should be a sample which does not show any thermal transition during the heating or cooling and whose c_p is well-defined in the temperature range of the experiment (usually an empty capsule is used). As DSC is not an absolute measuring technique, calibration of the reference is essential. The reference and sample are in independet compartments, as it can be seen in figure 2.8. [28] [29].

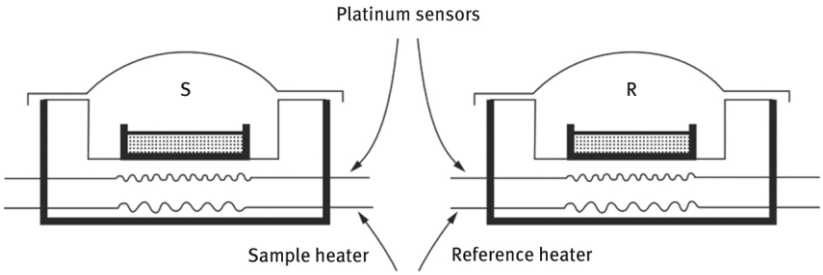

Figure 2.8. Schematic of DSC.[27]

Each sample is heated or cooled at the same rate and the calorimeter maintains identical the temperature of the two samples during the process. To maintain the same temperature in both samples DSC will exchange heat with them. Applying the difference between the heat flow of the reference and the sample under investigation, which are calculated with equations 2.1 and 2.2, it is obtained a diagram which expresses the heat flow in front of the temperature. The heat flow difference between the sample and the reference will be bigger when a phase transition is happening since to maintain the same temperature in the two samples more heat will be need to be observed or throwed out.[30,31]

This technique enables to determinate basic thermal properties related with melting, crystallization, glass transition or other processes that involve a change in the heat capacity or latent heat. Depending

on the mood of operation, isothermal crystallization or non-isothermal crystallization, different parameters are measured. [29]

In **non-isothermal** crystallization, crystallization temperature is not constant during the process and it drops with a constant cooling rate. From this type of crystallization phase transition temperatures, enthalpies and other thermal parameters can be determined.

Melting and crystallization are first order phase transitions so in a DSC scan, where heat flow is represented versus the temperature, a peak will be seen for the melting, which is an endothermic process and an inverse peak will be seen for the crystallization, which is an exothermic process. This is shown in the figure 2.9. Therefore, melting temperature, T_m and crystallization temperature, T_c, will be a maximum and minimum respectively.

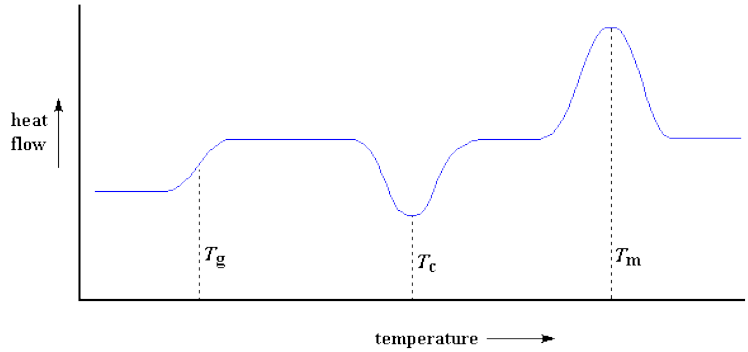

Figure 2.9. DSC scan where melting, crystallization and glass transition processes are distinguished.

Another two important parameters are melting enthalpy, ΔH_m, and crystallization enthalpy, ΔH_c. This two parameters expresses the heat exchanged in each process, so it can be calculated by an integration of the heat flow function.

As it has been mentioned before, most of the polymers are semycristalline, and it is very important to know the proportion between crystalline and amorphous materia which it is quantified with the crystallinity degree, X_c, which will determine strongly the physical properties of a polymer. In spite of been the same polymer, a difference in the X_c will change a lot the final properties.

Melting and crystallization are inverse processes, so if the two transitions are performed under the same conditions melting enthalpy and crystallization enthalpy should have the same absolute value. Therefore, X_c can be calculated with the following equation:

$$Xc = \frac{\Delta H_m}{\Delta H_m^\circ} \ (\boldsymbol{Eq.2.3})$$

ΔH_m is the total melting enthalpy measured experimentally for a polymer while ΔH_m° is the equilibrium melting entalphy, which is theoretically the enthalpy that would be obtained from the melting of a 100% crystalline sample. Thus, T_m°, ΔH_m° only can be calculated doing an extrapolation of several experimental measures of ΔH_m and X_c. If the measured ΔH_m is high, crystallinity degree will be higher too because it means that more heat has been needed to melt the crystalline structure.[32]

Glass transition temperature behaves like a second order phase transition, so in a DSC scan instead of appearing a maximum or a minimum, as in the case of T_m and T_c, an inflexion point will be seen (Figure 2.9) . Apart from that, T_g is usually much more lower than T_m and T_c so the experiment should be done in another temperature range.

In **isothermal crystallization**, crystallization temperature is maintained constant during the crystallization. From this type of process overall kinetics can be studied with the determination of $\tau_{\%50}$ and applying Avrami and LH theories.

Related with the melting, another important thermal parameter is equilibrium melting temperature, T_m°, which is the melting temperature of an infinite stack of extended chain crystals. As it has been explained in the introduction, kinetics dominates the crystallization of a polymer rather than thermodynamics, so actually this kind of infinite long lamellaes do not exist. Therefore, this parameter cannot be measured directly and it is needed to do an extrapolation.

For the extrapolation different procedures exist and one of them is Hoffman-Weeks. According to this procedure $T_m°$ will be the point at which an extrapolation of the experimental melting temperatures that have been measured during an isothermal crystallization and a $T_m=T_c$ line crossed. This is not an extremely accurate process but due to its simple procedure it is widely used.[33]

2.2.2.2 Experimental Procedure

Experiments were performed using a DSC Perkin Elmer 8000 calorimeter, which can be seen in the figure 2.10. The DSC was equipped with a refrigerated cooling system Intracooler 2P, under a nitrogen atmosphere (with a flow of 20 mL/min) and calibrated with high purity indium and tin standards. The weight of the samples was between 4 and 5 mg and samples were hermetically sealed in standard aluminum pans. For the determination of the T_g a Perkin Elmer 8500 calorimeter was used to achieve a faster cooling rate.

Figure 2.10. DSC Perkin Elmer 8000 calorimeter that was used in the lab.

For the non-isothermal crystallization, the same procedure of the PLOM has been used but after doing one melting and cooling a second melting has been done too. Second melting is needed to obtain thermal parameters related to the melting since the objective of the first melting is erase the previous thermal history and it is not reliable to obtain results from that first melting.

To measure the glass transition temperature a different protocol and DSC was used, since T_g is much more lower than T_c and T_m. The procedure was the same as in the non-isothermal crystallization but it was used ballistic cooling, which is the fastest cooling rate that can achieve the DSC and this cooling was done until -90°C. Glass transition is a phase transition that happen in amorphous structures. Because of that, it is important to do the cooling faster so that glass transition is more visible in the DSC scan.

It is important to do the cooling faster so the sample is more amorphous and as glass transition is a phase transition that happen in amorphous structures, the curvature change will be more visible in the DSC scan.

Isothermal crystallization experiments were performed, following the procedure suggested by Lorenzo et al.[34] The protocole was similar to the employed with the PLOM, since results obtained from two experimental techniques want to be comparable:

1) Heat the sample at 20°C/min until 90°C and stay 3 minutes at that temperature in order to erase previous thermal history of the polymer.
2) Cool down at 60°C/min until the choosen crystallization temperature. DSC could achieve 60ºC/min cooling rate while PLOM maximum cooling rate was 50ºC, that is why different cooling rates have been used.
3) Stay at the T_c variable times: between 15 and 60 minutes depending on the temperature, 15 minutes for the lowest T_c and 60 minutes to the highest T_c.
4) Heat again at 20°C/min until to 90°C to erase the previous thermal history.
5) Repeat the same procedure to have in total at least 5 T_c. for each homopolymer.

To choose which T_c was used for the isothermal crystallization first of all was determined the minimun crystallization temperature, $T_{cmin,}$ of each polymer. This parameter is the temperature at which start the crystallization during a cooling scan. The following procedure was applied:

1) Heat the sample at 20°C/min until 90°C and stay 3 minutes

2) Cool down at 60°C/min until a crystallization temperature.
3) As soon as it was arrived to the T_c melt the sample and repeat the procedure for 10-15 crystallization temperatures.

T_{cmin} was the lowest temperature at which no heat exhanged was appreciated.

2.2.3 Transmission Electron Microscopy (TEM)

2.2.3.1 Theoretical basis

TEM is a microscope that use electrons to visualize an object. It is used to analyze with a smaller scale than a usual optical microscope, since this last one is limited due to the wavelength of the visible light. The structure of the TEM can be simply explained by the figure 2.11:

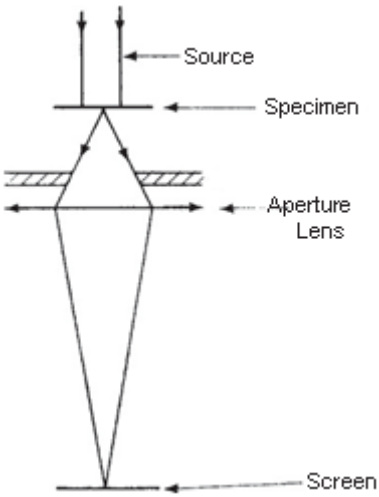

Figure 2.11. Schematic of a simple TEM.[35]

Electrons are emitted by the source and are accelerated before arriving to the sample so that the wavelength of the electron decrease and its energy increase. Between the electrons and material different interaction can happen: some electrons will pass through the sample without any interaction,

some of them will be scattered and others will be absorbed by the sample. If the sample is crystalline, the electrons are diffracted by planes of atoms inside the material, as happens for x-rays. It is therefore possible to form a transmission electron diffraction pattern from electrons that have passed through a thin specimen. Because of that, TEM will differentiate crystalline and amorphous domains, so it is a good option for the study of polymer.[35]

Another two important parts of this analytical instrument are the aperture of the lens. The aperture of the imaging lens will determine which scattered electrons will form the image. If the electrons used to form the image are the deflected ones it will be formed an image of Dark-field, where the amorphous areas will be of dark color whereas if the electrons used are the undeflected ones the image will be Bright-field, where the areas of brighter color will be the amorphous ones. Finally, a scintillator is used to convert the electrons to light pulses so that an image an image will be seen in the screen. With a device is possible to project the image in a computer. [36]

In the images obtained by TEM, lamellaes between amorphous material will be seen so this images can be used to measure lamellae thickness, although it is not the most accurate method.

2.2.3.2 Experimental procedure

Analysis and micrographs of the four homopolymers by the TEM were done by an external group. However, as the sample has to be an ultrafine layer to be able to be analyzed by the TEM, firstly the sample was prepared in the linkam equipment in form of thick film to be later cryo-cut and stained. For that, first of all, T_{cmin} of each sample was determined doing cooling processes and seeing if any crystal was formed before it arrives to the T_c.

After the determination of the T_{cmin}, the sample was prepare putting a little bit less sample quantity than in the samples that were analyzed by the PLOM. After that, the sample was heated and cooled with a rate of 20°C/min in both cases until the previously determined T_{cmin} and was let there some minutes to ensure the crystallization of the sample.

2.2.4 Wide-Angle X-ray scattering (WAXS)

2.2.4.1 Theoretical Basis

X-ray is a type of electromagnetic radiation with a short wavelength, between 0.01 and 10 nm, and high energy. Therefore it is used to determine in a smaller scale the structure of the polymer crystal and the position of the atoms in the unit cell. As other types of electromagnetic radiation, different phenomenon can happen when X-ray attack the sample, and one of them is scattering, as happen in the TEM.

When X-rays attack a solid material rays are scattered in many directions, but if the atoms are in an ordered way, that is, if the solid is crystalline, the rays can scatter in an exact direction, which it is known as diffraction of X-rays. This phenomenon happens according to the Bragg law, which is described in the equation 2.4:

$$2dsin\theta = n\lambda \ (\boldsymbol{Eq.2.4})$$

Where d is the interatomic distance of two crystallographic planes, Θ is the angle of incidence, which is the same as the angle of scattering, n is an integer number and λ is the wavelength. Bragg´s law describe the condition for an X-ray to be diffracted by a family of lattice planes.

Depending on the measurement of the diffracted angle there exist two types of X-ray scattering techniques: WAXS, Wide Angle X-ray Scattering, where 2Θ is wider than 1° whereas SAXS, Small Angle X-ray Scattering, where 2Θ is smaller than 1°. For both techniques the equipment is similar, as it can be seen in the figure 2.12, but as in WAXS wider angles are measured the detector is placed closer to the sample.[37]

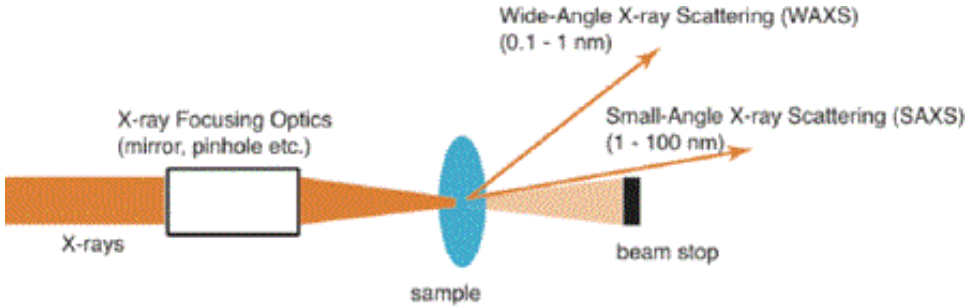

Figure 2.12. Schematic of WAXS and SAXS measurements.[37]

2.2.4.2 Experimental procedure

WAXS experiments were carried out by SGIker service in Bilbao. For the measurement Bruker D8 Advance diffractometer operating at 30 kV and 20 mA, equipped with a Cu tube (λ = 1.5418 Å), a Vantec-1 PSD detector, and an Anton Parr HTK2000 high-temperature furnace were used. The powder patterns were recorded in 2θ steps of 0.033º in the 5 ≤2θ ≤ 38 range, counting for 2s per step (total time for each temperature 39min). Data sets were recorded at different temperatures using 0.166 °C s-1 heating rate.

3-RESULTS AND DISCUSSION

3.1 PLOM

3.1.1 Non-isothermal crystallization

This type of crystallization have done to see in general the behaviour and morphology of crystals under non-isothermal conditions. In the figure 3.1 can be seen micrographs taken at 25°C of each homopolymer after a non-isothermal crystallization.

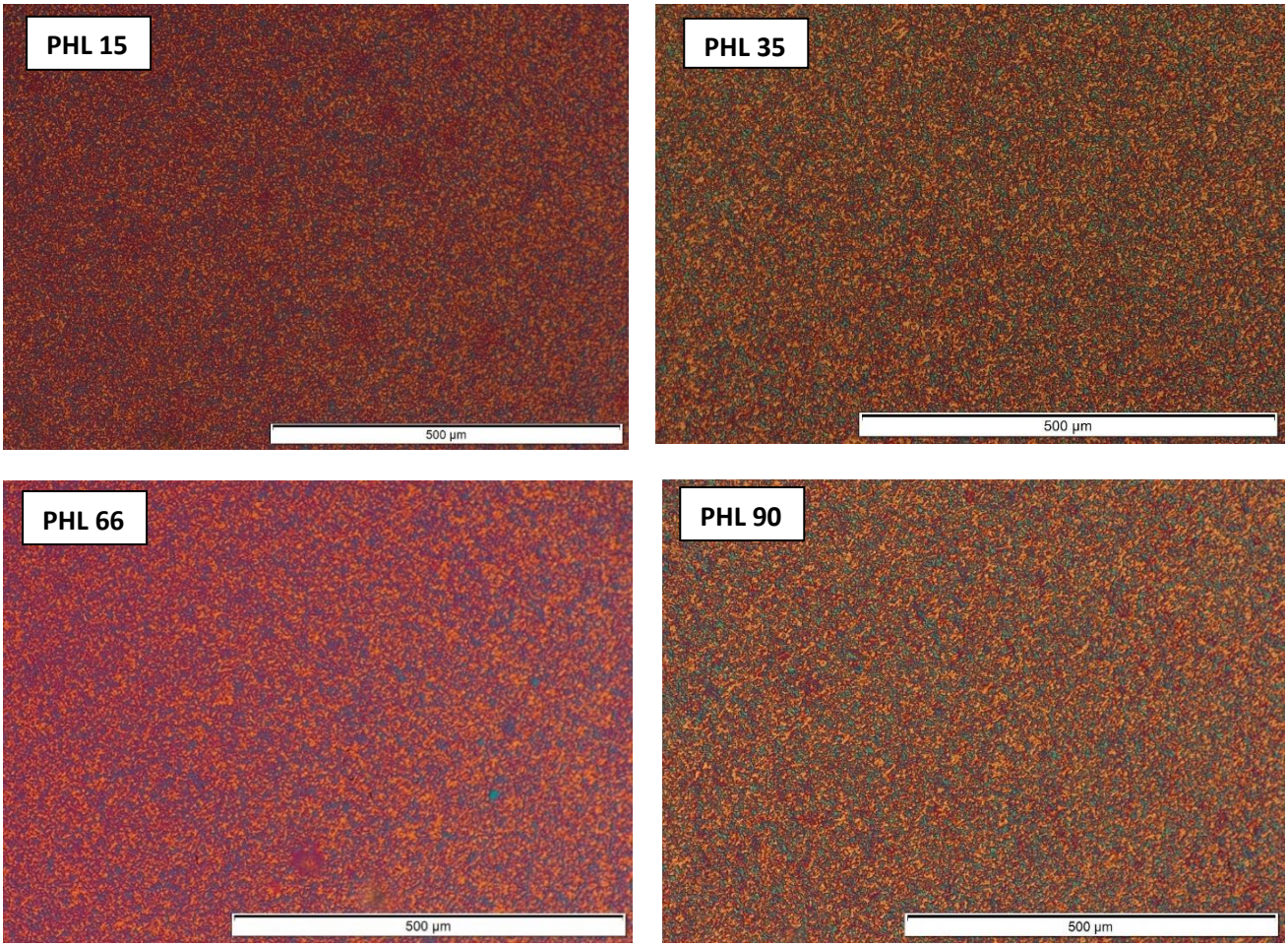

Figure 3.1 PLOM micrographs at 25°C after cooling from the melt at a rate of **50°C/min**.

As it can be seen in figure 3.1 there are several and very small crystals that have impinged between them during the cooling scan. However, these results are not very useful since is not appreciated the morphology of the crystals and the size of the crystals is very small.

3.1.2 Isothermal crystallization

Morphology can be better apreciated from isothermal crystallization results. In fact, as the crystallization is performed at a constant temperature, less crystals but bigger ones are formed as it can be seen in figure 3.2. This micrographs were taken after 3 minutes of isothermal crystallization at the same supercooling, ΔT, which is the difference between T_m and T_c. ΔT was 5°C; in the case of PHL 15 at 50°C, PHL 35 at 53°C, PHL 66 at 56°C and PHL 90 at 57°C.

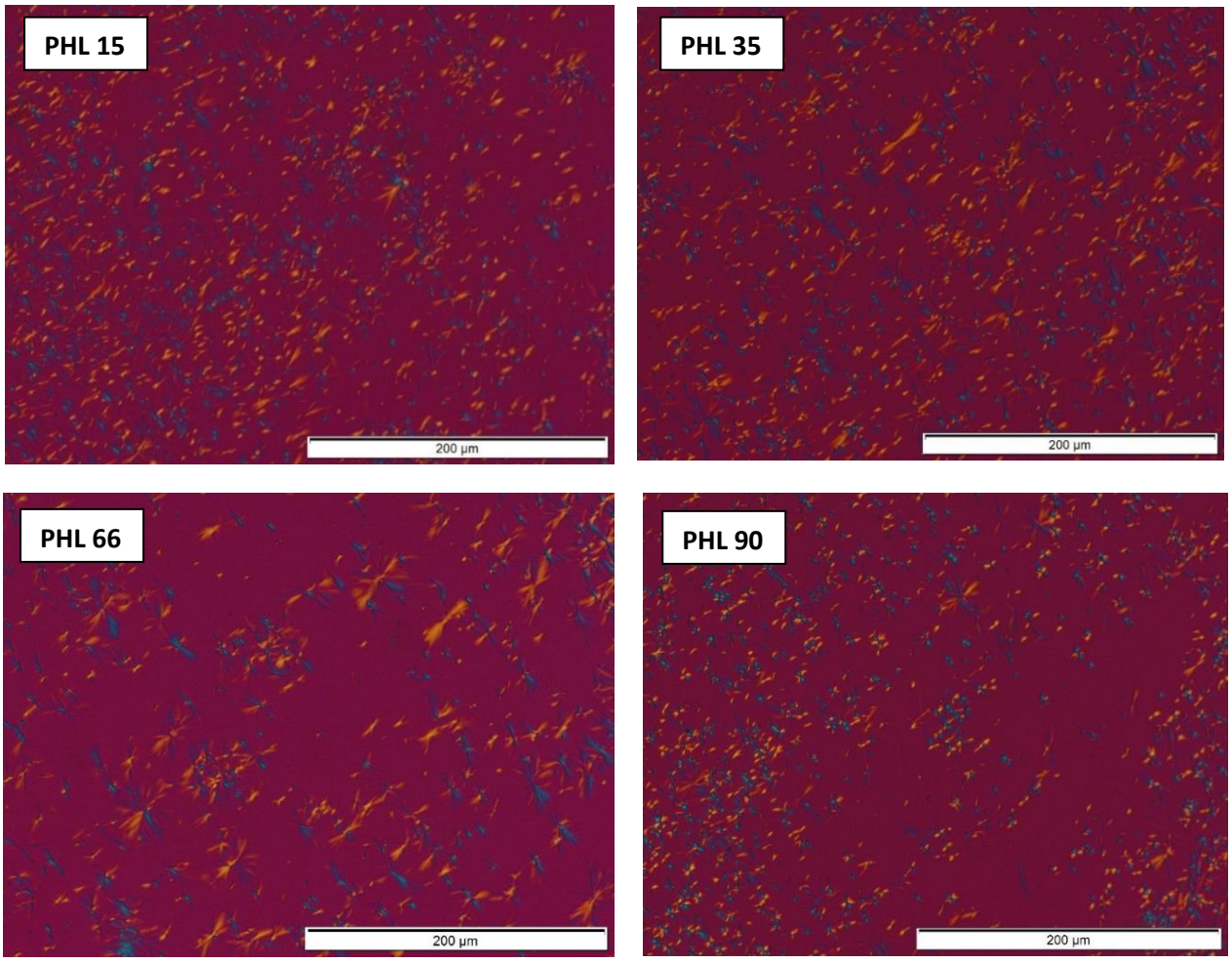

Figure 3.2. Morphology of crystals formed during isothermal crystallization at ΔT=5°C

However it can be seen that the crystalline structures are not the typical spherulites since instead of having a circular shape they have a kind of extended form. Therefore, they seems to be axialites instead of spherulites.

Following the crystallization growth with the PLOM it can be determinated the type of primary nucleation: sporadic or instantaneous. Looking at micrographs of the figure 3.2, there are crystals of different size. Thus it is clear that nucleation is sporadic and all the nucleis do not appear at the same time and with the pass of the time new nucleis appear.

Crystallization growth kinetics of four homopolymers have been studied measuring the size of the crystals at different times. In this case crystals do not have the typical circular shape so instead of measure the radius the length from one extreme to the other one has been measured. It has to be remark that crystal density of the four homopolymers was high while crystals were quite small so the measure of spherulites has been a little bit problematic. Because of that, zones with less density were searched and it was tried to measure crystals before they collapsed with each other.

In order to calculate G, the length of the crystals has been represented in front of the time at different temperatures, like it can be seen in the figure 3.3, which are the results of eight different T_c for PHL 15. Points are the experimental data whereas lines are the lineal fit that has been applied. The slope of each function is G. Experimental data fits a linear function, so it is believed that G is constant.

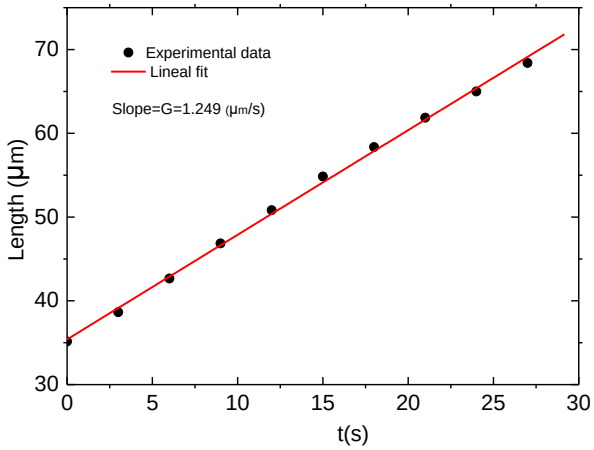

Figure 3.3. Graphic of crystal length at different times in order to calculate G. Data of PHL 15 at 46ºC

G has been calculated for each temperature and each homopolymer, and the results are in the following table:

Table 3.1. Results of the G at each crystallization temperature for each polymer.

PHL 15	**T_c (°C)**	46	47	48	49	50	50.5	51	52
	G (µm/s)	1.25	0.700	0.515	0.379	0.145	0.108	0.0656	0.0408
PHL 35	**T_c (°C)**	50	51	52	53	53.5	54	54.5	55
	G (µm/s)	0.840	0.519	0.328	0.240	0.184	0.125	0.0565	0.0271
PHL 66	**T_c (°C)**	53	54	55	56	56.5	57	57.5	58
	G (µm/s)	0.473	0.323	0.263	0.152	0.119	0.0406	0.0212	0.0154
PHL 90	**T_c (°C)**	54	55	56	57	58	59	60	61
	G (µm/s)	0.641	0.325	0.215	0.147	0.0950	0.0684	0.0578	0.0494

In order to study nucleation kinetics, LH fit of experimentally obtained G has been done using the free Origin plug-in developed by Lorenzo et al.[34] and important graphics and parameters have been obtained from it. One of them is the theoretical G values at a wider range of temperatures, applying LH equation, as it can be seen in the figure 3.4:

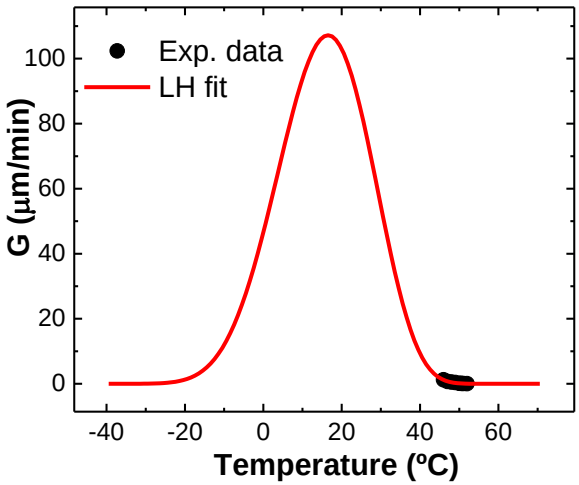

Figure 3.4. Experimental and theoretical values of G after LH fit for PHL 15.

The behaviour of the four homopolymers have been compared in figure 3.5, putting the data of four homopolymers Vs the crystallization temperatures used.

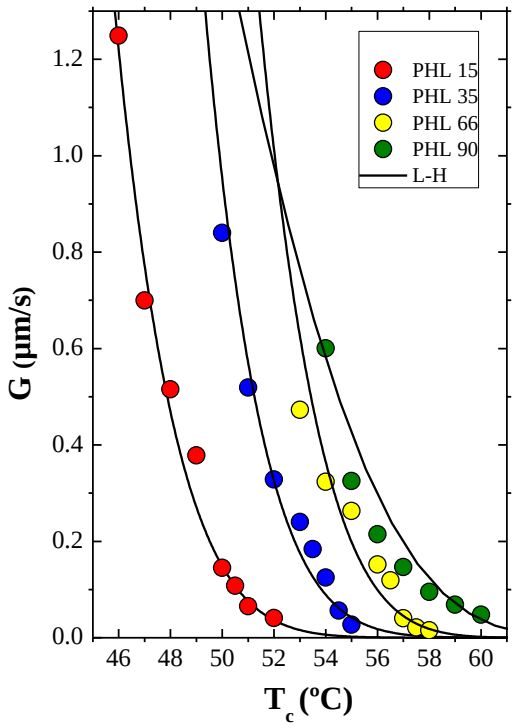

Figure 3.5. LH fit of the recorded experimental data of G in front of the T_c.

The four homopolymers behave similarly. The only one that differs a little bit is PHL 90, since its curve is different and even crosses with PHL 66 curve.

However, in the four homopolymers is clear one phenomenon: G decreases when the T_c is increased. What it means that at higher crystallization temperatures the Growth of the crystals is slower. As it has been explained in the introduction, G is dependant of molecular transport to the nuclei and the growth of the nuclei. Temperature affects oppositely each process, so graphics of G in front of temperature (between T_g and T_m) have bell shape and there is a temperature with a maximum G, as it is shown in the figure 3.4. Therefore, it means that the obtained experimental results are in the right side of the graphic. In fact, at higher temperatures there are not many activated nuclei and it is favoured the growth of these nucleis than the creation of new ones. This behaviour was expected as the employed T_c are nearer to the T_m than to the T_g.[10]

Comparing the four homopolymers the descendent curve is similar but happens at different temperature intervals. In fact, taking the same temperature for the four homopolymers G increases when M_n increases. This tendence is confirmed in the figure 3.6, where G values of four homopolymers taken at the same crystallization temperature, 54.5°C, have been represented in front of M_n.

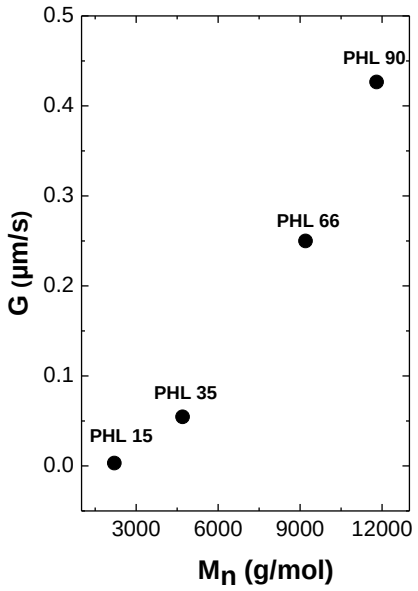

Figure 3.6. Comparison of G in front of M_n at a T_c of 54.5ºC

Apart from the G another important parameters, K_g, σ, σ_e and q, have been determined from the figure 3.7 and applying the Eq. 1.6. This has been obtained with the previously mentioned origin plug-in[34] where the LH fit is applied to the experimental data. The results are presented in the table 3.2:

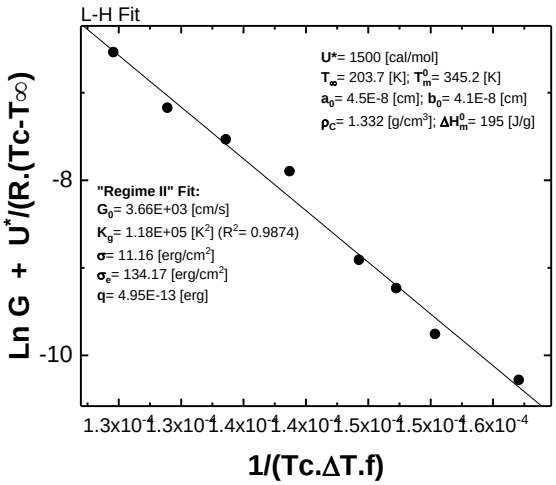

Figure 3.7. Linerization of G vs Tc graphic for PHL 15.

Table 3.2. Results of K_g, σ, σ_e, q and R.

	K_g	σ (erg/cm^2)	σ_e (erg/cm^2)	q (erg)	R
PHL 15	1.18 x 10^{+05}	11.16	134.17	4.95 x 10-13	0.9874
PHL 35	3.55 x 10^{+05}	11.16	131.74	4.86 x 10-13	0.9462
PHL 66	7.10 x 10^{+04}	11.16	80.61	2.97 x 10-13	0.9396
PHL 90	3.19 x 10^{+04}	11.16	36.33	1.34 x 10-13	0.9322

Analyzing the results, R, which is the is the correlation coefficient for the fitting of the LH equation, in the four cases is above 0.9000 and the one that fits better is PHL 15. K_g, which is a energy barrier related to the nuclei growth, decreases while M_n increases, resulting in a higher G value (Figure 3.6).

3.2 DSC

3.2.1 Non-isothermal crystallization

Doing non-isothermal crystallization experiments DSC scans of melting, crystallization and glass transition temperatures have been obtained, which can be seen in the figures 3.8 and 3.9. In that scans first and second order transitions, that is, maximums, minimums and inflexion points, are clearly seen so it is evident that the four homopolymers are semycristalline and no totally amorphous. However, in the case of glass transition the curvature change is no so clear, especially in the cases of PHL 66 and PHL 90. So it has been more difficult to measure accurately the inflexion point.

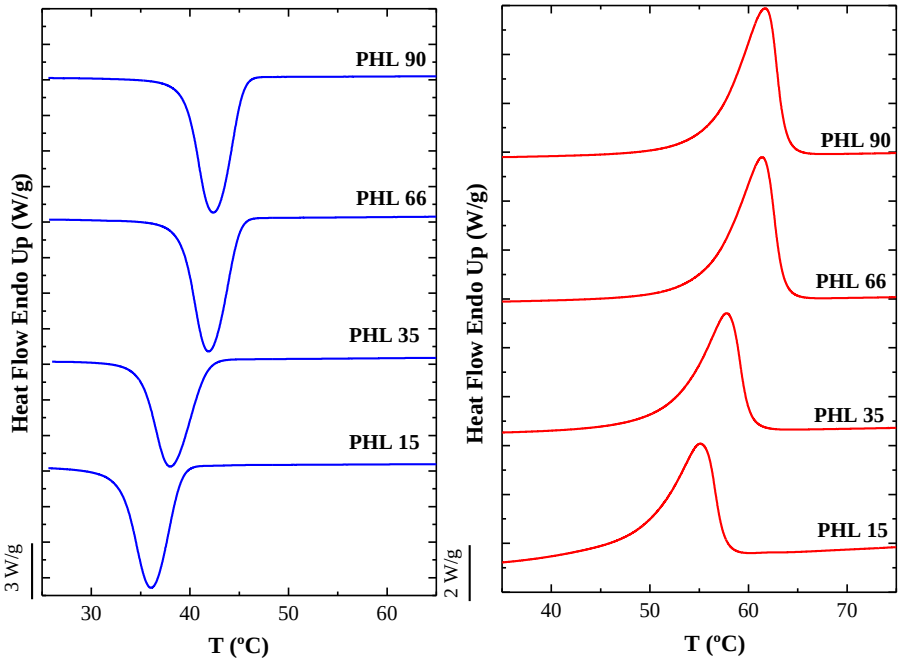

Figure 3.8 Crystallization and melting non-isothermal DSC scans.

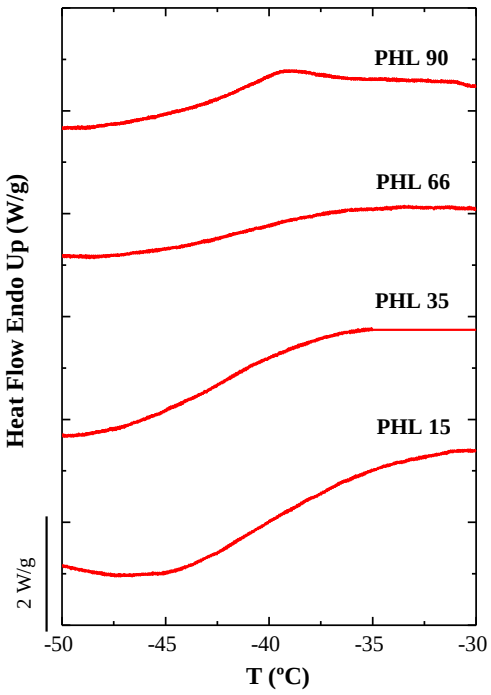

Figure 3.9 Glass transition non-isothermal DSC scan.

From that scans phase transition temperatures: T_m, T_c and T_g and enthalpies, ΔH_m and ΔH_c have been calculated and the results are shown in the table 3.3:

Table 3.3 Thermal parameters obtained from non-isothermal crystallization

	T_g (°C)	T_c (°C)	T_m (°C)	ΔH_c (J/g)	ΔH_m (J/g)	X_c
PHL 15	-39.3	36.1	55.1	-86	84	0.43
PHL 35	-42.5	38.0	58.8	-77	79	0.41
PHL 66	-41.1	41.9	61.3	-91	90	0.46
PHL 90	-39.7	42.3	61.7	-91	93	0.48

Analyzing T_m and T_c values it is clear that phase transition temperatures rise with M_n, as it shown in the figure 3.10. This behaviour is supported by Flory equation, which is shown in the equation 3.1, where T_m is the melting temperature, Tm^{∞} is the melting temperature of a infinite molecular weight, R is the gas constant, ΔH_{mu} is the heat of fusion per mole of the repeating unit and M_0 is the molecular weight of the repeating unit.

$$\frac{1}{T_m} - \frac{1}{T_m{}^{\infty}} = \frac{2RM_0}{\Delta H_{mu} M_n} \quad (\boldsymbol{Eq\ 3.1})$$

Flory equation states that T_m increases with number average molecular weight (M_n) and that can be extrapolated to other phase transition temperatures. That increase tends to stabilize as M_n rises and arrive to a maximum usually when M_n > 100 kg/mol.[38] Obtained T_m vs M_n graphic is a very good example of how the increase tends to stabilize with M_n. However looking at the obtained T_g results in the table 3.3, T_g does not rise with Mn. The reason might be that the inflexion point was no so clear in the DSC scans and probably in the measure some errors have been made. However, four T_g values are similar, between -39°C and -43°C.

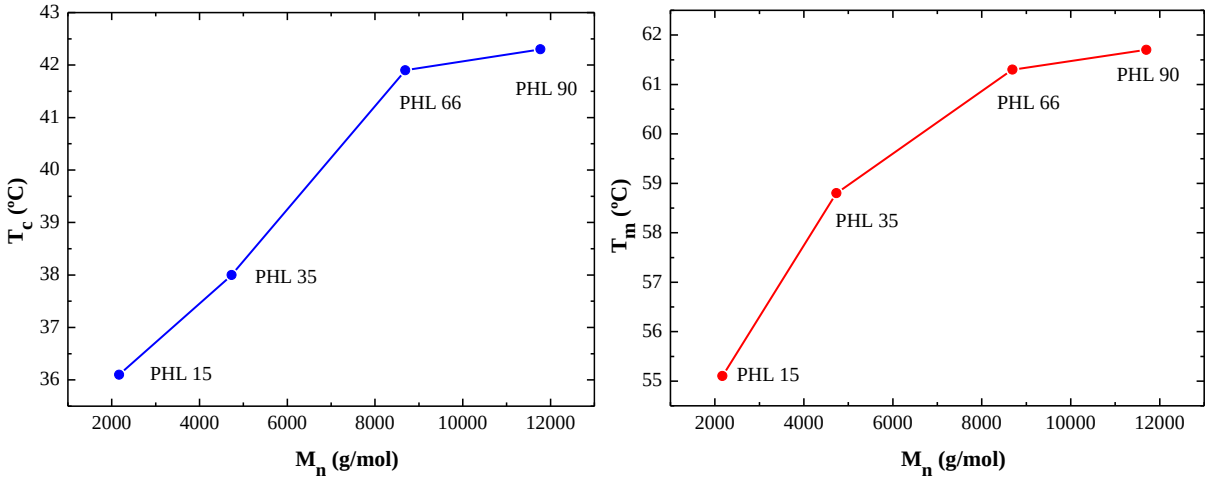

Figure 3.10 T_m and T_c in front of M_n. The solid lines represent an arbitrary fit to guide the eyes.

In the case of ΔH_m and ΔH_c, the four homopolymers show a similar absolute value with a difference of no more than 15 J/g between the highest one (PHL 90) and the smallest one (PHL 15), as it is shown in the table 3.3. Nevertheless, it is not seen a correlation between ΔH value and M_n in the results. Melting and crystallization are opposite processes so is theoretically supposed that absolute values of ΔH_m and ΔH_c should be identical if the crystalline structure has been melted totally. In each homopolymer ΔH_m and ΔH_c values are similar and the difference between them is less than 10%, so the results are acceptable.

X_c, can be calculated with the previously mentioned equation 2.3, where ΔH_m is dividided by $\Delta H_m°$. In order to calcualte $\Delta H_m°$ it was tried to get experimentally different ΔH_m and X_c values applying different cooling rates. However, despite using different cooling rates the values of ΔH_m and X_c obtained were very similar and they were not adequate to do an extrapolation. Therefore, ΔHm° has been calculated applying group contribution theory[39] and the value of ΔHm° is 195 J/g. Results of X_c are in the table 3.3. In the four homopolymers a similar X_c has been obtained, between 0.4 and 0.5.

3.2.2 Isothermal crystallization

Isothermal crystallization has been performed at different temperatures and cooling scans as can be seen in figures 3.11 and 3.12. Heat flow diagrams show very different curves at each temperature: the ones at low T_c are sharper more intense while the ones at higher T_m are wider but less pronounced. This can be related with the results of the PLOM. At lower temperatures growth rate was higher so at lower temperatures crystallization is faster and less time is needed. Therefore, the peak will be more intense and sharper.

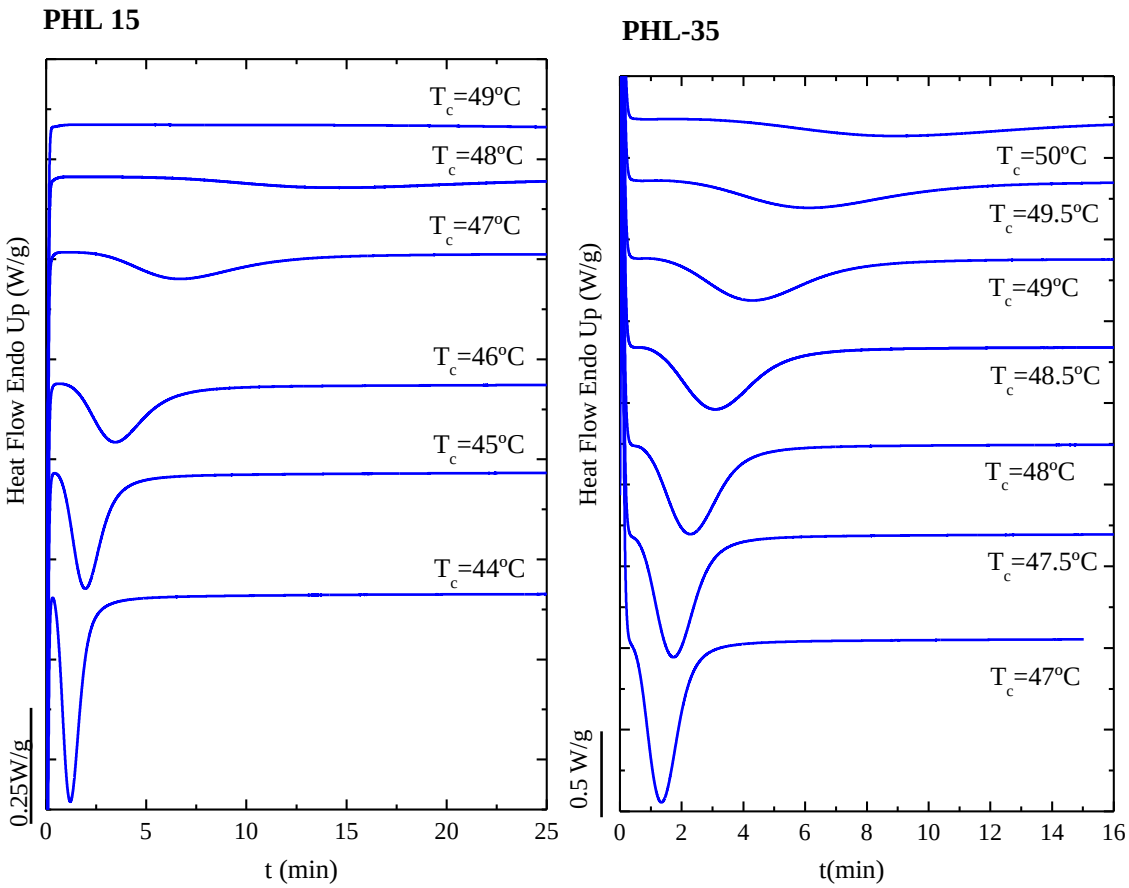

Figure 3.11 DSC scans of isothermal crystallization of PHL 15 and PHL 35

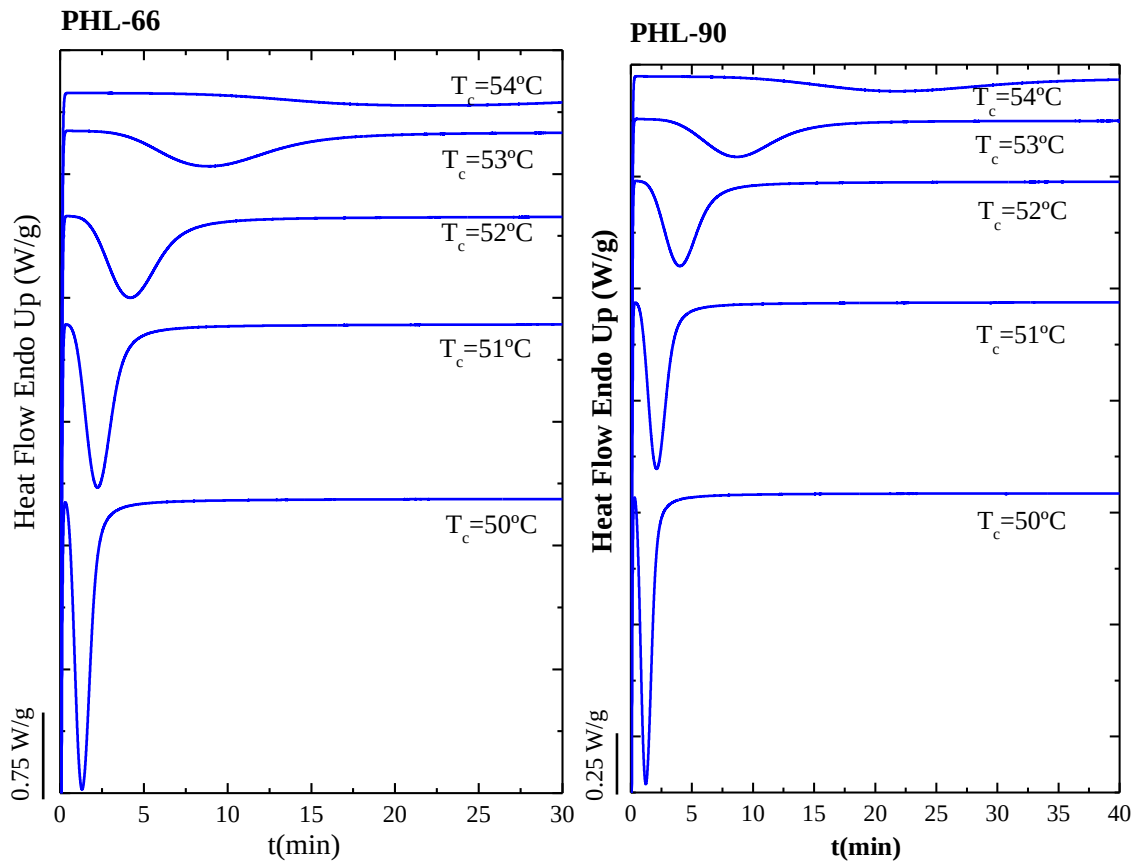

Figure 3.12. DSC scans of isothermal crystallization of PHL 66 and PHL 90

In order to analyse isothermal crystallization results the previously mentioned origin plug-in has been applied. With DSC results instead of using LH theory to analyse the results Avrami theory has been used. Using 1.2, 1.3, 1.4, 1.5 and 1.7 equations mentioned in the introduction, different graphics are obtained by the plug-in, which can be seen in the figure 3.13.

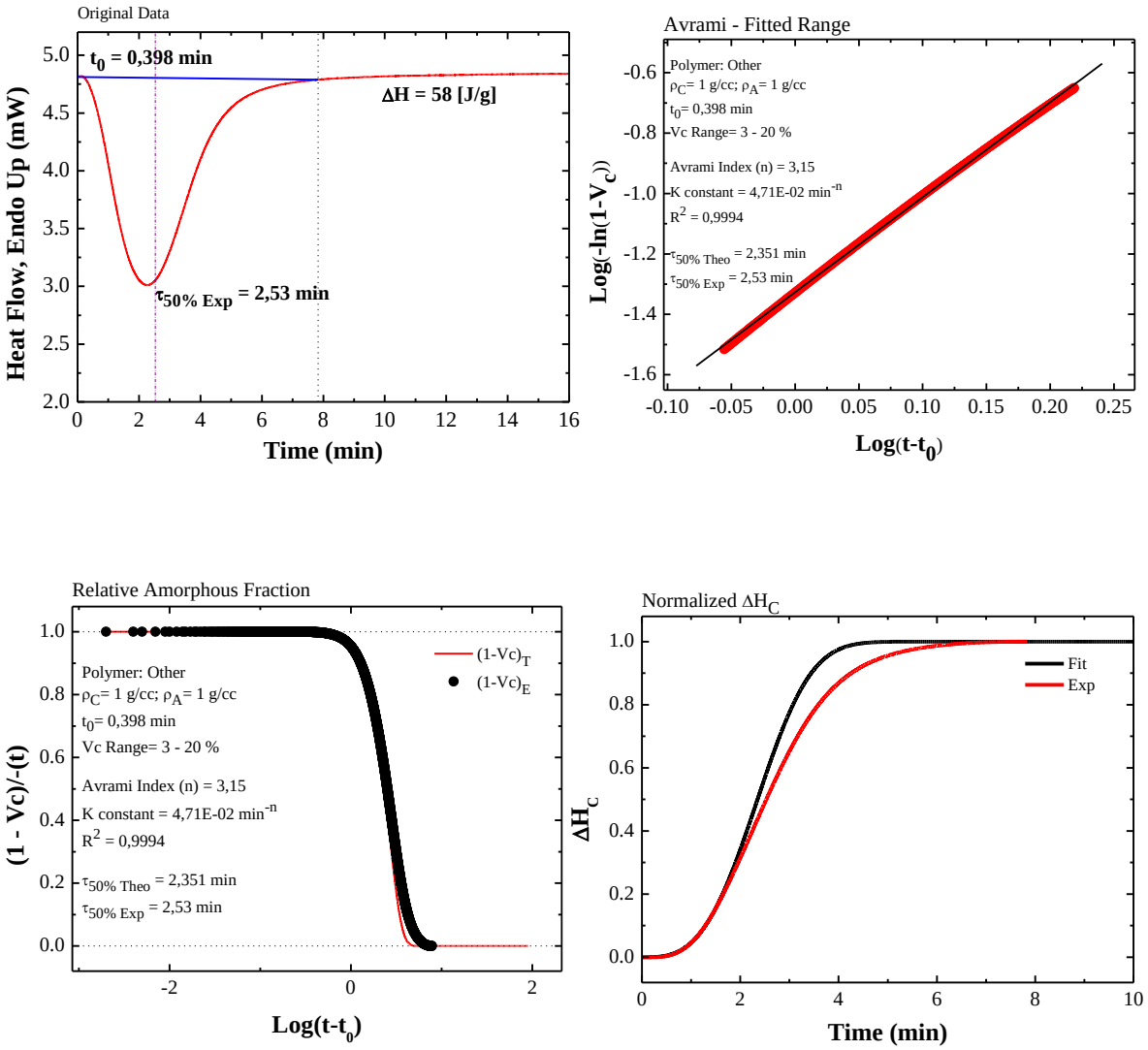

Figure 3.13. Different graphs obtained from origin plug-in for the PHL 35 at T_c 48°C

From graphics of the figure 3.13 main overall kinetics parameters have been obtained and the results are presented in the table 3.4, 3.5, 3.6 and 3.7.

Table 3.4 Overall kinetics parameters of **PHL 15**

T_c (°C)	t_0 (min)	n	K (min^{-n})	$K^{1/n}$ (min^{-1})	R	$\tau_{\%50E}$ (min)	$\tau_{\%50T}$ (min)
44	0.352	2.85	8.00×10^{-01}	0.925	1.000	0.951	0.978
45	0.440	3.14	1.37×10^{-01}	0.531	1.000	1.674	1.742
46	0.573	3.50	1.26×10^{-02}	0.287	0.999	3.140	3.327
47	1.638	3.04	3.80×10^{-03}	0.160	1.000	5.535	5.730
48	3.272	3.44	1.58×10^{-04}	0.0785	0.999	11.425	11.933
49	19.102	2.17	$1{,}23 \times 10^{-03}$	0.0456	1.000	18.504	18.646

Table 3.5. Overall kinetics parameters of **PHL 35**

T_c (°C)	t_0 (min)	n	K (min^{-n})	$K^{1/n}$ (min^{-1})	R	$\tau_{\%50E}$(min)	$\tau_{\%50T}$(min)
47	0.350	2.85	5.59×10^{-01}	0.815	1.000	1.079	1.092
47.5	0.418	2.95	2.47×10^{-01}	0.662	1.000	1.418	1.442
48	0.705	2.6	1.63×10^{-01}	0.498	0.999	1.745	1.743
48.5	1.007	2.52	8.24×10^{-02}	0.371	0.999	2.327	2.316
49	1.022	2.85	1.80×10^{-02}	0.244	1.000	3.599	3.656
49.5	1.848	2.58	1.23×10^{-02}	0.182	1.000	4.751	4.772
50	2.167	2.83	2.39×10^{-03}	0.118	1.000	7.394	7.563

Table 3.6. Overall kinetics parameters of **PHL 66**

T_c (°C)	t_0 (min)	n	K (min^{-n})	$K^{1/n}$ (min^{-1})	R	$\tau_{\%50E}$(min)	$\tau_{\%50T}$(min)
50	0.353	2.86	6.37×10^{-01}	0.854	1.000	1.036	1.054
51	0.413	3.31	7.56×10^{-02}	0.459	1.000	1.955	2.024
52	0.997	3.03	1.59×10^{-02}	0.255	1.000	3.471	3.555
53	2.237	2.96	1.97×10^{-03}	0.121	1.000	7.242	7.493
54	5.693	2.91	1.81×10^{-04}	0.0518	1.000	17.042	17.995

Table 3.7. Overall kinetics parameters of **PHL 90**

T_c (°C)	t_0 (min)	n	K (min^{-n})	$K^{1/n}$ (min^{-1})	R	$\tau_{\%50E}$(min)	$\tau_{\%50T}$(min)
50	0.353	2.75	7.94×10^{-01}	0.794	1.000	0.952	0.969
51	0.413	3.23	1.02×10^{-01}	0.102	1.000	1.810	1.640
52	0.705	3.37	9.98×10^{-03}	9.8×10^{-03}	1.000	3.519	3.627
53	1.647	3.37	7.70×10^{-04}	7.7×10^{-04}	1.000	7.507	7.736
54	5.985	3.01	1.40×10^{-04}	1.4×10^{-04}	0.999	16.901	16.922

On the one hand, in order to study overall crystallization kinetics, experimental $1/\tau_{\%50,}$ which is crystallization rate, has been represented in front of T_c, and the results are shown in the figure 3.14. In

the graphic it can be seen the obtained experimental $1/\tau_{\%50}$ while the black line represents the theoretical values obtained applying LH equation. It can be said that experimental data fits well LH fit.

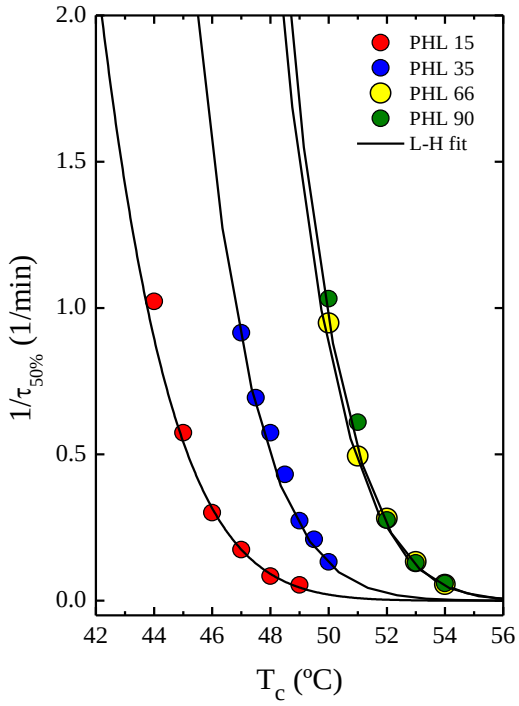

Figure 3.14. Crystallization rate at different T_c to study overall crystallization kinetics of each homopolymer.

When figure 3.14 and 3.5 are compared, it can be seen that two graphics are very similar with a decrease of G and $1/\tau_{\%50}$ when $T_{c\ is}$ increased. This behaviour was hoped since $1/\tau_{\%50}$ is related with overall crystallization kinetics which is influenced by G, that is related with crystal growth and I, which is related to primary crystallization. The only difference is appreciated in PHL 66 and PHL 90, since in the case of crystallization rate, figure 3.14, the obtained data is very similar and both curves almost overlap, while in the case of G, figure 3.5, the values are more different.

$1/\tau_{\%50}$ behaviour in front of M_n has been studied at a constant T_c of 47°C, which can be seen in the figure 3.15. Similar to the figure of G vs Mn, figure 3.6, crystallization rate increases as M_n is increased.

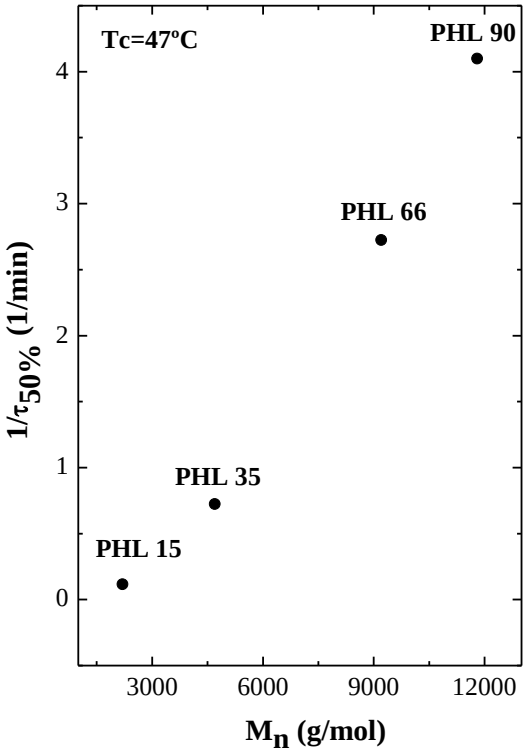

Figure 3.15. Comparison of $1/\tau_{\%50}$ in front of M_n at a T_c of 47°C.

On the other hand, primary crystallization can be also analyzed representing in this case nucleation rate, $1/t_0$ in front of T_c, as it can be seen in the figure 3.16. For the same T_c a higher nucleation rate is measured when M_n increased.

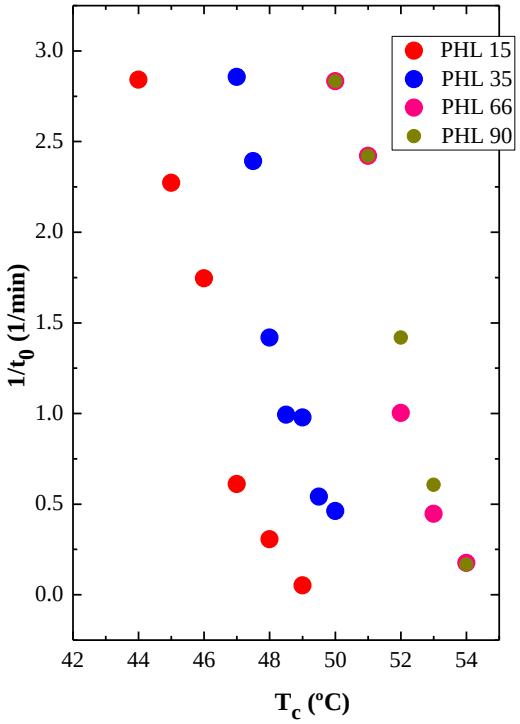

Figure 3.16. Study of primary nucleation representing $1/t_0$ vs T_c

As it is shown in tables 3.4, 3.5, 3.6, 3.7, apart from $\tau_{\%50}$ and $t_{0,}$ another kinetics parameters have been calculated, such as avrami index. Obtained n values are between 2 and 3.5, depending on the polymer and T_c. Overall avrami index is calculated by the sum of n_d and $n_{n.}$ From micrographs of the PLOM, it was clear that all the nucleis did not created at the same time so the nucleation was sporadic and n_n has to be higher than 0. However, with the dimension were some doubts and it is not sure if axialites or spherulites are formed, what would involve a n_d of 2 or 3 respectively.

Analyzing k results, it is seen that k value decrease with the T_c, what it is hoped in a process that happens at low supercooling (nearer to the T_m than to the T_g), where the process is dominated by the nucleation instead of by the molecular transport. R^2, which is the correlation coefficient for the fitting of the avrami equation in the double-logarithmic plot, is above 0.9990 in all cases, so the fit is regarded as very good in the chosen conversion range.[10]

During the isothermal crystallization a subsequent melting scan has been done also and the results of each homopolymer can be seen in the figure 3.17:

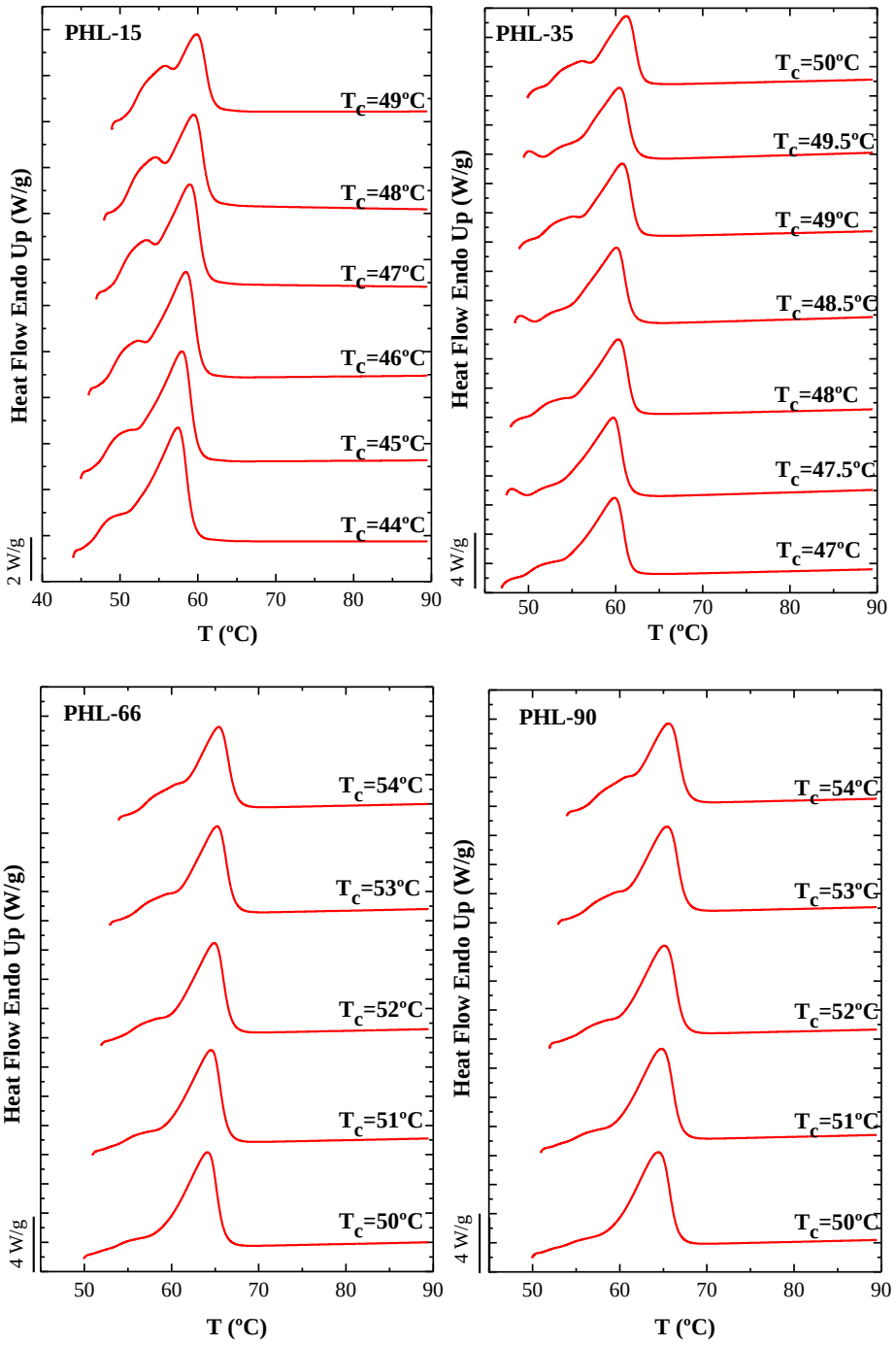

Figure 3.17. Subsequent melting plots of each polymer crystallized at different T**c**.

In this case the heat flow curves are no so perfect as in the crystallization and although there is a main peak, there is an additional smaller peak too at lower temperatures, especially in the case of PHL 15. Melting scan during an isothermal crystallization is very useful to calculate $T_m°$, equilibrium melting

temperature, which has been calculated employing Hofmann-Weeks process. As it can be seen in the figure 3.18, the temperature at which the extrapolation of recorded T_m and the line T_c=T_m cross is T_m°.

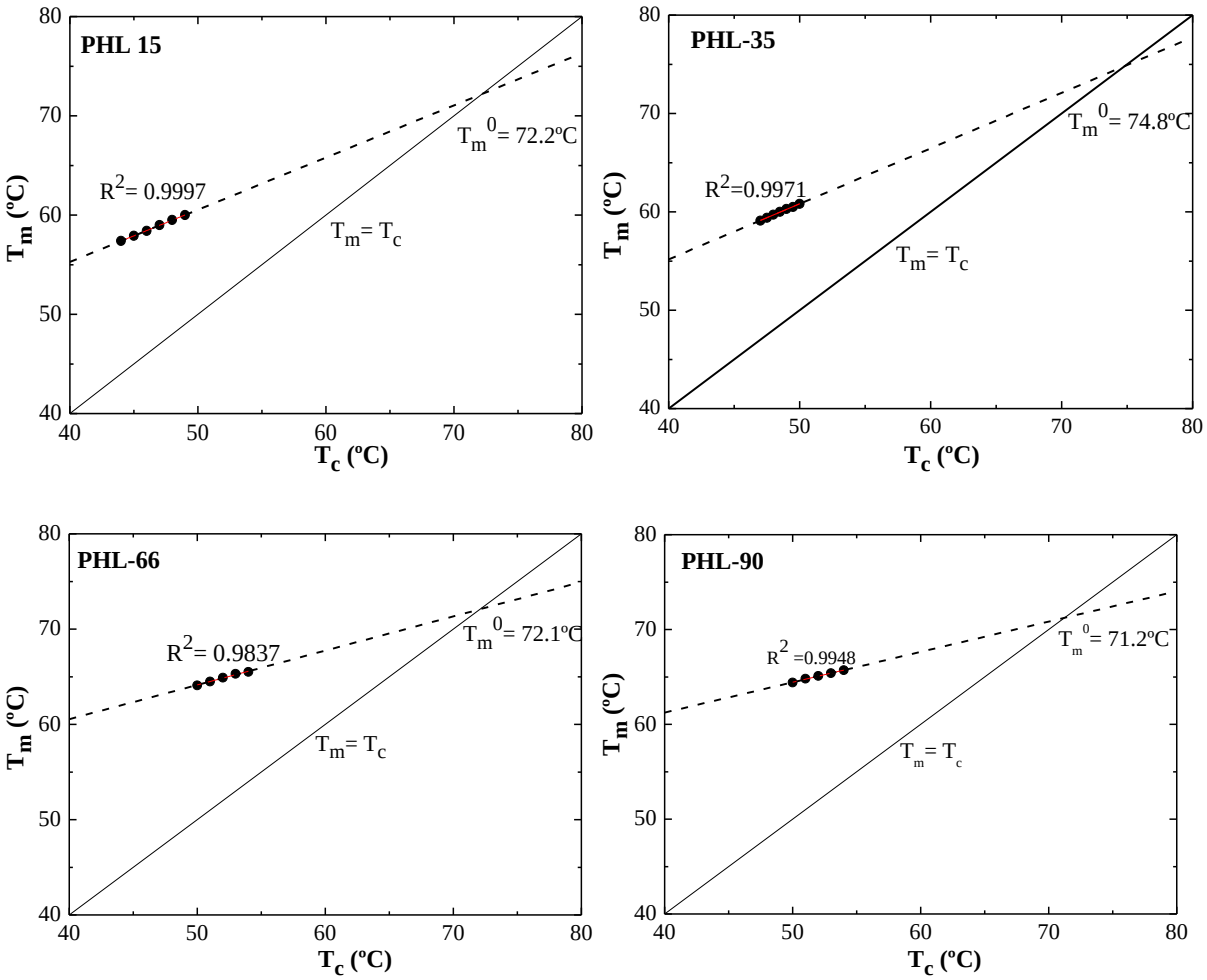

Figure 3.18. Extrapolation of Hofmann-weeks in order to calculate T_m°.

Analyzing the results, there is no an expected direct correlation between T_m° and M_n as happened with T_m and T_c. The reason could be that the extrapolation have been done in a very wide range of temperature, since the difference between recorded T_m and T_m° is about 20°C, so it is more likely to happen an error. However, the four homopolymers have a quite similar T_m° value between 71°and 74°C as it is shown in the table 3.8. Besides, this value is similar to the T_m° of PCL, which is estimated to be 78°C.[40]

Table 3.8. Results of $T_m°$ calculating by the extrapolation of Hofmann-weeks.

	PHL 15	PHL 35	PHL 66	PHL 90
$T_m°$ (°C)	72.2	74.8	72.1	71.2

3.3 TEM

TEM technique has been applied for each homopolymer, but useful micrographs where lamellae structure is distinguished have been obtained only with PHL 15 and PHL 35. Probably because the samples of PHL 66 and PHL 90 were not as thin as they should to be able to be analyzed by TEM. Results for PHL 15 and PHL 35 are shown in the figures 3.19 and 3.20.

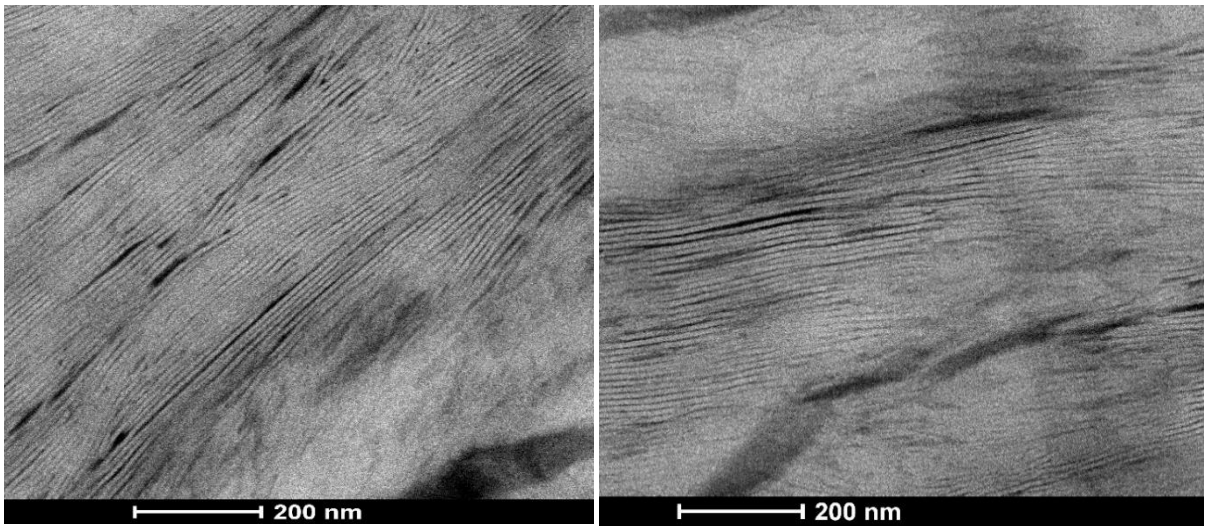

Figure 3.19. Micrograph obtained after doing TEM for PHL 15 where lamellaes can be distinguished.

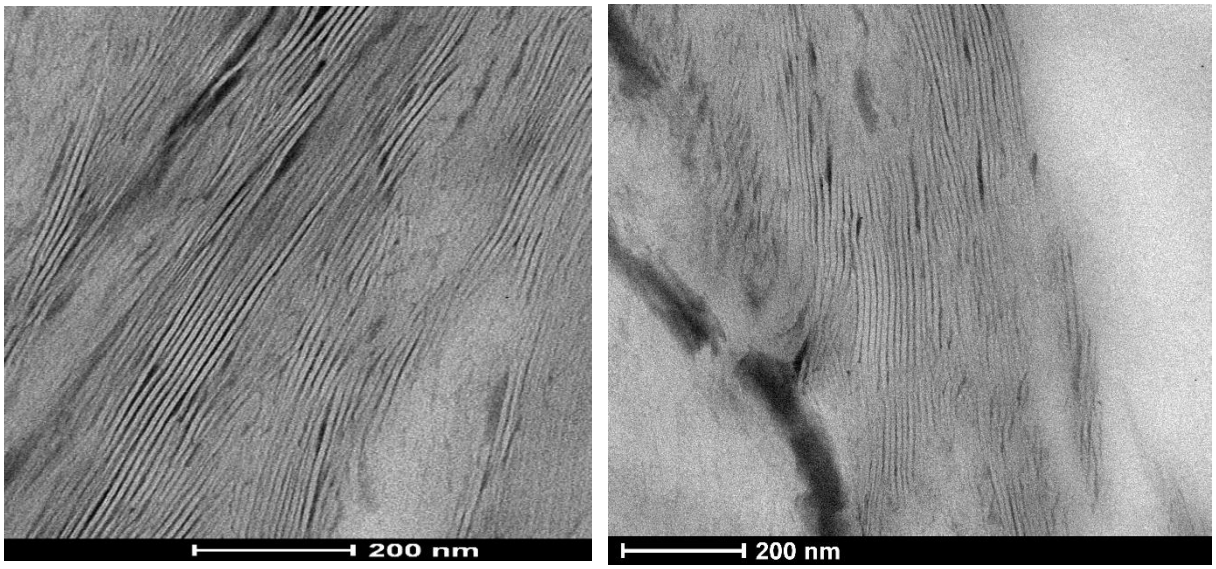

Figure 3.20. Micrograph obtained after doing TEM for PHL 35 where lamellaes can be distinguished.

In those micrographs are distinguished darker and brigther areas. In this case Black Field type of TEM has been employed so black areas are formed of amorphous materia while grey or brighter ones are formed of crystalline materia. In fact, in those crystalline areas can be distinguish some lines which delimitate the lamellae. Therefore, lamellae thickness has been measured manually from that micrographs using Image J programme. For each homopolymer 100 measurements have been done and the thickness distribution graphics are shown in the figure 3.21.

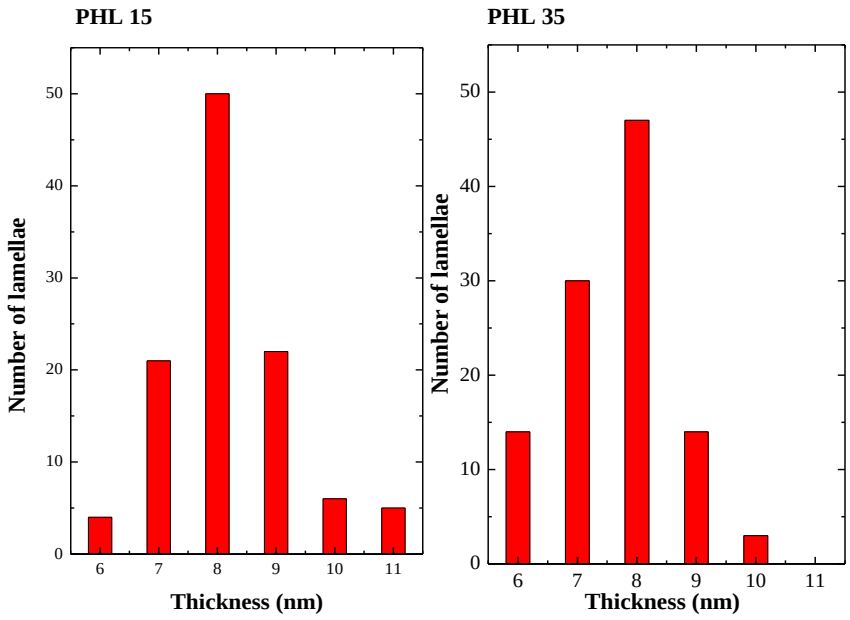

Figure 3.21. Distribution of the measured lamellae thickness of PHL 15 and PHL 35

Lamellae thickness is very similar in both homopolymers with a number average thickness of around 8nm. This value is comparable to some values obtained for ultrathin PCL films.[41]

3.4 WAXS

From WAXS experiments the following diffractograms have been obtained, which represents the intensity of the scattering X-ray in front of 2Θ, the double of the scattering angle.

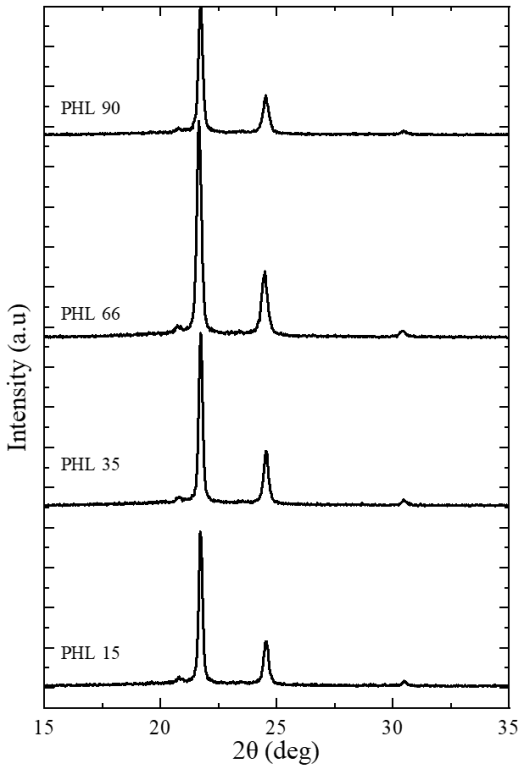

Figure 3.21 WAXS diffractogram of four homopolymers

The four homopolymers show two signals of scattering at the same 2Θ angle value, between 20º and 25º, one more intense than the other. As the four homopolymers have the same repeated unit, atoms are organized identically in the crystal unit cell so the X-rays are scattered with the same angle. However the intense of each diffractogram is quite different. More intense signals should appear in samples with higher crystallinity degree, since X-ray scattering happens in crystalline regions. In this

case, PHL 66 seems to have the most intense signal although from the results of the DSC it was determined that the most crystalline polymer was PHL 90.

Comparing with diffractograms of PCL in the literature, PHL x-ray diffraction happens at the same 2Θ angle values, what it was hoped since the repeating unit of each polymer is very similar with the only difference of one additonal carbon in the case of PHL.[42]

4-CONCLUSIONS

- The polymers under investigation, PHL 15, PHL 35, PHL 66 and PHL 90, are stable and can endure crystallization experiments. DSC, PLOM, TEM and WAXS results confirms that four polymers are semicrystalline.

- Some properties and parameters depends on the molecular weight while others do not. DSC results shows that phase transitions temperatures are affected by the molecular weight since melting temperature and crystallization temperature increase when molecular weight is increased. In addition, overall crystallization kinetics and growth kinetics are affected by the M_n in the same way, since crystallization and growth rate increases while molecular weight is increased.

- However, some properties and parameters are not affected by the molecular weight. TEM micrographs show lamellaes between amorphous materia and its thickness do not change with the molecular weight. In the same way, WAXS diffractograms shown that four homopolymers have the same crystal unit cell.

- Isothermal crystallization at the DSC and PLOM have shown that crystallization kinetics (Overall and growth) are dominated by nuclei growth since Crystallization rate and Growth rate decrease with the rise of T_c.

- PLOM results shows that crystals do not have the typical circular shape of spherulites. They have an extended form, so it is believed that they are axialites.

4-ONDORIOAK

- Aztertu diren polimeroak, PHL 15, PHL 35, PHL 66 eta PHL 90, egonkorrak dira eta kristalizazio esperimentuak jasan ditzazkete. DSC, PLOM, TEM eta WAXS bidez lortutako emaitzak polimeroak erdi-kristalinoak direla konfirmatzen dute.

- Propietate eta parametro batzuk pisu molekularraren menpean daude eta beste batzuk aldiz ez. DSC bidez lortutako emaitzak pisu molekularrak fase trantzisio tenperaturetan eragiten duela adierazten dute. Izan ere, fusio eta kristalizazio tenperaturak handitzen dira pisu molekularraren igoerarekin batera. Pisu molekularrak ere kristalizazio osoko zinetika eta hazkuntza zinetika baldintzatzen ditu, kristalizazio eta hazkuntza abiadurak pisu molekularraren igoerarekin batera handitzen baitira.

- Hala ere, propietate eta parametro batzuk ez dira aldatzen pisu molekularraren arabera. TEM bidez lortutako argazkiak lamelak materia amorfoaren tartean erakusten ditu eta lamela hauen lodiera ez da aldatzen pisu molekularrarekin. Aldi berean, WAXS bidez lortutako difraktogramek lau homopolimeroek kristal egitura berdina dutela adierazten dute.

- DSC eta PLOM-ren bidez egindako kristalizazio isotermikoak, kristalizazio zinetika (Osoa eta Hazkuntza) nukleoaren hazkuntzak dominatzen duela adierazten du. Izan ere, kristalizazio eta hazkuntza abiadurak jeisten dira kristalizazio tenperaturaren igoerarekin batera.

- PLOM-ren emaitzek kristalak ez dutela esferuliten forma zirkular tipikoa adierazi dute. Horren ordez, forma luzaxka bat dute eta horregatik axialitak direla uste da.

5-REFERENCES

(1) Pilla, S. *Handbook of Bioplastics and Biocomposites Engineering Applications*; John Wiley and Sons, 2011.

(2) European Bioplastics e.V. https://www.european-bioplastics.org/ (accessed Jun 16, 2021).

(3) Ezgi Bezirhan Arikan; Havva Duygu Ozsoy. A Review: Investigation of Bioplastics. *J. Civ. Eng. Archit.* **2015**, *9* (2), 188–192.

(4) Albertsson, A.-C.; Varma, I. K. Aliphatic Polyesters: Synthesis, Properties and Applications. In *Degradable Aliphatic Polyesters*; 2002; pp 1–40.

(5) Vroman, I.; Tighzert, L. Biodegradable Polymers. *Materials (Basel).* **2009**, *2* (2), 307–344.

(6) Polyesters https://www.essentialchemicalindustry.org/polymers/polyesters.html (accessed Jun 18, 2021).

(7) Ilustración del Polycaprolactone (PCL) https://www.stocklib.es (accessed Jun 18, 2021).

(8) Labet, M.; Thielemans, W. Synthesis of Polycaprolactone: A Review. *Chem. Soc. Rev.* **2009**, *38* (12), 3484–3504.

(9) Van Der Mee, L.; Helmich, F.; De Bruijn, R.; Vekemans, J. A. J. M.; Palmans, A. R. A.; Meijer, E. W. Investigation of Lipase-Catalyzed Ring-Opening Polymerizations of Lactones with Various Ring Sizes: Kinetic Evaluation. *Macromolecules* **2006**, *39* (15), 5021–5027.

(10) Cavallo, D.; Müller, A. J. Polymer Crystallization. In *Macromolecular Engineering*; 2019.

(11) Mark, J. *Physical Properties of Polymers Handbook Second Edition*; 2007.

(12) Polymer Crystallinity The amorphous nature of polymers. https://slidetodoc.com/polymer-crystallinity-the-amorphous-nature-of-polymers-is/ (accessed Jun 24, 2021).

(13) Spherulites and optical properties https://www.doitpoms.ac.uk/tlplib/polymers/spherulites.php (accessed Jun 18, 2021).

(14) Gránásy, L.; Pusztai, T.; Douglas, J. F. Insights into Polymer Crystallization from Phase-Field Theory. In *Encyclopedia of Polymers and Composites*; Springer Berlin Heidelberg, 2013; pp 1–35.

(15) Reiter, G.; Sommer, J.-U. *Polymer Crystallization: Observations, Concepts and Interpretations*; 2003; Vol. 608.

(16) Soto, D. TFG. Estudio de La Cristalización y de La Transición de Brill En El Nylon 5,6, Universitat Politècnica de Catalunya, 2009.

(17) Androsch, R.; Schick, C. Crystal Nucleation of Polymers at High Supercooling of the Melt. *Adv. Polym. Sci.* **2017**, *276*, 257–288.

(18) Di Lorenzo, M. L.; Silvestre, C. Non-Isothermal Crystallization of Polymers. *Prog. Polym. Sci.* **1999**, *24* (6), 917–950.

(19) Wang, Z. G.; Hsiao, B. S.; Sauer, B. B.; Kampert, W. G. The Nature of Secondary Crystallization in Poly(Ethylene Terephthalate). *Polymer (Guildf).* **1999**, *40* (16), 4615–4627.

(20) Zhou, L.; Wang, Z.; Zhang, M.; Guo, M.; Xu, S.; Yin, Q. Determination of Metastable Zone and Induction Time of Analgin for Cooling Crystallization. *Chinese J. Chem. Eng.* **2017**, *25* (3), 313–318.

(21) Pérez, R. Phd. Crystallization and Morpholgy of Multiphasic Polymeric Systems: Random Copolymers, Nanocomposites and Polymers with Complex Chain Topologies, UPV/EHU, 2019.

(22) Guo, Q. *Polymer Morphology: Principles, Characterization, and Processing*; 2016.

(23) Williams L. Solid State Properties Chapter 4. https://slideplayer.com/slide/7057461/ (accessed Jun 28, 2021).

(24) White, R. P.; Lipson, J. E. G. Polymer Free Volume and Its Connection to the Glass Transition. *Macromolecules* **2016**, *49* (11), 3987–4007.

(25) The Glass Transition https://pslc.ws/macrog/tg.htm (accessed Jun 28, 2021).

(26) Piorkowska, E.; Rutiedge, G. C. *Handbook of Polymer Crystallization*; 2013.

(27) Abd-Elghany, M.; Klapötke, T. M. A Review on Differential Scanning Calorimetry Technique and Its Importance in the Field of Energetic Materials. *Phys. Sci. Rev.* **2018**, *3* (4).

(28) Wunderlich, B. *Thermal Analysis of Polymeric Materials*; 2005.

(29) Schick, C. Differential Scanning Calorimetry (DSC) of Semicrystalline Polymers. *Analytical and Bioanalytical Chemistry*. Springer November 14, 2009, pp 1589–1611.

(30) Richardson, M. The Application of Differential Scanning Calorimetry to the Measurement of Specific Heat. In *Compendium of Thermophysical Property Measurement Methods*; 1992.

(31) Sandoval, A.; Rodriguez, E.; Fernandez, A. Aplicación Del Análisis Por Calorimetría Diferencial de Barrido (DSC) Para La Caracterización de Las Modificaciones Del Almidón. *Dyna* **2005**, *72* (146), 45–53.

(32) Kong, Y.; Hay, J. N. The Measurement of the Crystallinity of Polymers by DSC. *Polymer (Guildf).* **2002**, *43* (14), 3873–3878.

(33) Marand, H.; Xu, J.; Srinivas, S. Determination of the Equilibrium Melting Temperature of Polymer Crystals: Linear and Nonlinear Hoffman-Weeks Extrapolations. *Macromolecules* **1998**, *31* (23), 8219–8229.

(34) Lorenzo, A. T.; Arnal, M. L.; Albuerne, J.; Müller, A. J. DSC Isothermal Polymer Crystallization Kinetics Measurements and the Use of the Avrami Equation to Fit the Data: Guidelines to Avoid Common Problems. *Polym. Test.* **2007**, *26* (2), 222–231.

(35) Egerton, R. F. *Physical Principles of Electron Microscopy: An Introduction to TEM, SEM, and AEM*; Springer US, 2005.

(36) Klein, T.; Buhr, E.; Frase, C. G. TSEM: A Review of Scanning Electron Microscopy in Transmission Mode and Its Applications. In *Advances in Imaging and Electron Physics*; 2012.

(37) Kumar, R.; Austin, L.; Kumar, R.; Kousar, B.; Lampadaris, C. H.; Lucas, M. M. *SAXS and WAXS Measurements of Polyethylene Terephthalate (PET)*; 2018.

(38) Müller, A. J.; Saenz, G.; Salazar, J. Crystallization of PLA-Based Materials. In *Poly(lactic acid) Science and Technology: Processing, Properties, Additives and Applications*; 2015.

(39) Van Krevelen, D. W.; Nijenhuis, K. *Properties of Polymers*; Elsevier, 1997.

(40) Chen, H. L.; Li, L. J.; Ou-Yang, W. C.; Hwang, J. C.; Wong, W. Y. Spherulitic Crystallization Behavior of Poly(∈-Caprolactone) with a Wide Range of Molecular Weight. *Macromolecules* **1997**, *30* (6), 1718–1722.

(41) Yu, X.; Wang, N.; Lv, S. Crystal and Multiple Melting Behaviors of PCL Lamellae in Ultrathin Films. *J. Cryst. Growth* **2016**, *438*, 11–18.

(42) de Campos, A.; Tonoli, G. H. D.; Marconcini, J. M.; Mattoso, L. H. C.; Klamczynski, A.; Gregorski, K. S.; Wood, D.; Williams, T.; Chiou, B. Sen; Imam, S. H. TPS/PCL Composite Reinforced with Treated Sisal Fibers: Property, Biodegradation and Water-Absorption. *J. Polym. Environ.* **2013**, *21* (1), 1–7.